Palaeogeography, Palaeoclimatology, Palaeoecology 442 (2016) 72–83

Contents lists available at ScienceDirect

Palaeogeography, Palaeoclimatology, Palaeoecology

journal homepage: www.elsevier.com/locate/palaeo

Central Mediterranean Mid-Pleistocene paleoclimatic variability and its association with global climate

Lucilla Capotondi [a,*], Angela Girone [b], Fabrizio Lirer [c], Caterina Bergami [a,d], Marina Verducci [e], Mattia Vallefuoco [c], Angelica Afferri [b], Luciana Ferraro [c], Nicola Pelosi [c], Gert J. De Lange [f]

[a] CNR, Istituto Scienze Marine (ISMAR), Via Gobetti 101, 40129 Bologna, Italia
[b] Dipartimento di Scienze della Terra e Geoambientali, Università di Bari Aldo Moro, Italy
[c] CNR, Istituto per l'Ambiente Marino Costiero (IAMC), Calata Porta di Massa, Interno Porto di Napoli, 80133 Napoli, Italy
[d] CNR, Institute of Agro-environmental and Forest Biology (IBAF), Italy
[e] Dipartimento di Scienze della Terra, Università di Siena, Italy
[f] Department of Earth Sciences, Geochemistry, Faculty of Geosciences, Utrecht University, Netherlands

ARTICLE INFO

Article history:
Received 24 February 2015
Received in revised form 2 November 2015
Accepted 13 November 2015
Available online 24 November 2015

Keywords:
Planktonic foraminifera
Middle Pleistocene
Central Mediterranean
Paleoceanographic changes

ABSTRACT

Planktonic foraminiferal assemblages were studied at high-resolution in core KC01B from the Ionian Sea. Quantitative analysis allowed us to distinguish the main climatic features and associated paleoceanographic changes, that occurred between Marine Isotopic Stages (MIS) 13 and 9 (~500–300 ka).

MIS 12 and MIS 10 are characterized by relatively temperate conditions and an oligotrophic oceanographic regime in the early part and by colder conditions and nutrient supply in the sub-surface water masses in the upper part. During these intervals, small but distinct peaks of *Neogloboquadrina pachyderma* sinistral (sin) are detected at times of extremely negative values of the planktonic foraminifera paleoclimatic curve. Their co-occurrence with similar episodes in the Atlantic suggests that the climate in the Central Mediterranean was associated with north-Atlantic millennial-scale climate instability. MIS 11 and MIS 9 are dominated by surficial warm-water taxa. The climate optimum is reached in the middle part of each of these stages, as denoted by the presence of *Globigerinoides sacculifer*, and persists for approximately 20 and 6 ka during MIS 11 and MIS 9 respectively. This warming is not constant but is characterized by three distinct intervals with elevated winter temperatures and/or weak winter mixing.

Distribution of *Globigerina bulloides*, *Turborotalita quinqueloba* and *N. pachyderma* dextral (dex) indicates that significant environmental changes occur across the transitions from glacial to interglacial MIS 12/MIS 11 (Termination V) and MIS 10/MIS 9 (Termination IV).

The studied record documents a close linkage between Mediterranean climate evolution and higher- and lower-latitude climate change throughout MIS 13–9.

1. Introduction

To improve our understanding of natural climate variability and our abilities to forecast future climate change, it is essential to investigate geological climate archives with relevant climate change events. Accordingly, this paper focuses on climate variability that occurred before and after the Mid-Brunhes event (MBE) (Jansen et al., 1986) in the Mediterranean Sea. The investigated time interval (MIS 13–MIS 11; ~500–300 ka) is characterized by substantially warmer interglacials, (EPICA community members, 2004; Jouzel et al., 2007) and enhanced atmospheric CO_2 content, at levels similar to those for the pre-industrial Holocene (Siegenthaler et al., 2005). In particular, it includes the MIS 11c, traditionally considered as potential analogue for future climate evolution because of relatively similar orbital climate forcing (Loutre, 2003; Masson-Delmotte et al., 2006; Tzedakis et al., 2012). Therefore, a thorough study of this interval will provide information on type and magnitude of climate variability under non-anthropogenic but otherwise comparable conditions to the present.

In addition, the studied interval also includes the MIS 12, the most extreme glacial of the last 500 ka (Shackleton, 1987; Rohling et al., 1998; Lisiecki and Raymo, 2005) characterized by a sea level of about 125 m lower than today (Rohling et al., 2009, 2014). The MIS 12–11 transition (Termination V) is also part of this peculiar interval. It represents a glacial–interglacial transition that is long compared to later Pleistocene terminations (Oppo et al., 1998; Bauch et al., 2000; Thunell et al., 2002; Kandiano and Bauch, 2007; Helmke et al., 2008).

Notwithstanding the huge literature about the aforementioned climatic intervals, some features deserve additional clarifications. Two of the most intriguing aspects are the protracted deglaciation during

* Corresponding author.
E-mail address: lucilla.capotondi@bo.ismar.cnr.it (L. Capotondi).

http://dx.doi.org/10.1016/j.palaeo.2015.11.009
0031-0182/

Termination V and the cause of a long period of interglacial warmth during the MIS 11 (longer than any other mid-to late Pleistocene interglacial) with contrasting SST dynamics between polar- and mid-latitudes (Helmke and Bauch, 2003; Kandiano and Bauch, 2007; Kandiano et al., 2012; Milker et al., 2013 and references therein).

These issues could be addressed by analysing paleo-data from the Mediterranean Sea, a region highly sensitive to atmospheric and climatic system modifications due to its intermediate latitudinal position, where Euro-Asian and North-African climate regimes strongly interact (Roether et al., 1996; Béthoux et al., 1999; Pinardi and Masetti, 2000; Trigo et al., 2004; Lionello et al., 2006).

Moreover the Mediterranean climate is exposed to the South-Asian Monsoon in summer and the Siberian High-Pressure-System in winter (Luterbacher and Xoplaki, 2005; Lionello et al., 2006). Today, the southern part of the Mediterranean region is mostly influenced by the descending branch of the Hadley cell, while the northern part is more linked to mid-latitude variability, characterized by the North-Atlantic Oscillation (NAO) and other mid-latitude teleconnection patterns (Hurrel et al., 2004).

Thus, climate investigations of geological archives of the Mediterranean region reflect paleo-changes in the intensity and extension of global-scale climate patterns. In addition, the Mediterranean sedimentary sequences are characterized by the (quasi-) periodical occurrence of episodes of deep-sea oxygen depletion (sapropel layers) (Olausson, 1991; Rohling et al., 2015 and references therein). Based on their link with the astronomical parameters (Rossignol–Strick, 1983; Hilgen, 1991; Lourens, 2004; Konijnendijk et al., 2014) these discrete levels represent a useful constraint to establish accurate age models for marine and land sections.

We present a new high-resolution quantitative study of planktonic foraminifera distribution throughout MIS 13–9 for sediment core KC01B collected in the Ionian Sea, central Mediterranean Sea. Planktonic foraminifera are amongst the most commonly used proxies for paleoceanographic and paleoclimate sea-surface reconstructions. Their distribution and abundance are strongly linked to surface-water properties. In addition, the physical and chemical properties of their shells reflect past environmental conditions of the water masses in which they lived (Kucera, 2007 and references therein).

The investigated deep-marine sequence of core KC01B represents a key site for stratigraphic and paleoclimatic investigations. This is not only because of its strategic location but also because it was used for the construction of a sapropel-based astronomical timescale for the last 1.1 My (Lourens, 2004). Moreover, in this work, we update the studied time interval by using the recent chronological constraints on Pleistocene sapropel deposition (Konijnendijk et al., 2014) and a new oxygen isotopic record of *N. pachyderma*.

Our main aim is to explore how the ecosystem responded to climate variability during glacial and interglacial intervals throughout MIS 13–9 in order to discuss the possible mechanisms through which climate acts at the regional and global scale.

In detail, we focus on the main environmental and paleoceanographic processes occurring a) at times of glacial and interglacial MIS; b) during Termination V (T-V) and Termination IV (T-IV).

2. Modern oceanographic setting

Currently, the Mediterranean Sea is an evaporative basin where freshwater loss exceeds freshwater input, forcing an anti-estuarine circulation (Borghini et al., 2014).

At the surface (the first 100–200 m), moderate-salinity Atlantic Water (AW) intrudes through the Strait of Gibraltar and flows to the easternmost part of the Levantine basin modifying its temperature and salinity properties (Modified Atlantic Water—MAW). In the intermediate layer (depth between 150–200 and 600 m), Levantine Intermediate Water (LIW) forms in the eastern basin, spreads westwards and continues its flow towards the Strait of Gibraltar, and then into the Atlantic Ocean (Robinson et al., 1991; Béthoux et al., 1992; Manca et al., 2004; Malanotte-Rizzoli et al., 2014).

Atmospheric forcing and basin topography determine a large number of local cyclonic and anticyclonic cells (Pinardi and Masetti, 2000). In wintertime, outbreaks of cold and dry continental air masses lead to significant negative heat budgets and buoyancy losses, initiating deep and/or intermediate dense water formation both in the western and in the eastern basins (Malanotte-Rizzoli and Bergamasco, 1991; Castellari et al., 2000).

The Ionian Sea is influenced by the transit and on-site transformation of the major water masses previously described (e.g., Modified Atlantic Water, MAW; Levantine Intermediate water, LIW; and Eastern Mediterranean Deep Water, EMDW, Napolitano et al., 2000; Malanotte-Rizzoli et al., 2014) (Fig. 1). At the near-surface level, most important for biological production, the MAW enters in the western Ionian basin advected by the Atlantic Ionian Stream (AIS) (Fig. 1). Recently, the upper-layer circulation in the Ionian Sea has been associated with the deep thermohaline circulation through the Bimodal Oscillating System (BiOS): the Ionian upper-layer circulation reverses from cyclonic to anticyclonic and vice versa on decadal time scale affecting the biological productivity in the northern Ionian and southern Adriatic Sea (Civitarese et al., 2010; Gačić et al., 2010).

The present-day Mediterranean Sea is characterized by oligotrophic conditions (Béthoux, 1979; Sarmiento et al., 1988). The main factor that controls the seasonal change in primary production is linked to the dynamics of the water column with increasing biomass in late winter/early spring and decreasing in summer (Antoine et al., 1995; Bosc et al., 2004; D'Ortenzio and Ribera d'Alcalà, 2009).

A significant West-East trophic gradient exists with nutrient depletion (mainly phosphorus) and a reduction in primary productivity in the eastern basin (Krom et al., 1991, 2010).

Moreover, primary productivity reflects the hydrological fragmentation due to mesoscale variability (D'Ortenzio and Ribera d'Alcalà, 2009).

An oligotrophic regime, characterized by a low production, occurs in summer, when a stable stratification takes place (Klein and Coste, 1984; Krom et al., 1992; Crispi et al., 1999; Allen et al., 2002). During this period, low standing stocks characterize surface waters with the dominance of predatory species. The Ionian planktonic foraminiferal association is generally dominated by *Globigerinoides ruber* pink (40–60%) and *G. ruber* alba (20–40%) with peaks of maximum abundance in the first 50 m of the water column (Pujol and Vergnaud Grazzini, 1995). Winter convection, and less frequently frontal zone migration or upwelling, brings nutrients into the photic zone (mesotrophic regime) (Klein and Coste, 1984). During winter, the assemblage is characterized by the dominance of grazing species such as *Globorotalia truncatulinoides* (50%) and by the presence of other non-spinose species such as *Globorotalia inflata* (20%), and *Globigerina bulloides* (8%). *Globigerinoides ruber alba* (8%) and *Hastigerina siphonifera* (7%) are also part of the association. In detail, *G. inflata* and *G. ruber alba* are more abundant in the first 100 m of the water column, while *G. truncatulinoides* peaks at 200 m water depth (Pujol and Vergnaud Grazzini, 1995).

The moderate mixing and ventilation processes, occurring during wintertime, bring the nutrients to the photic layer (Napolitano et al., 2000) as documented by the coccolithophorid occurrence in sediment traps collected in this area (Ziveri et al., 2000) and the satellite-derived surface chlorophyll concentration (D'Ortenzio and Ribera d'Alcalà, 2009). This hydrographic/oceanographic feature can also explain the presence of juvenile specimens of *G. inflata* and *G. truncatulinoides* in the surface layer (Pujol and Vergnaud Grazzini, 1995).

3. Sediment core

Sediment core KC01B was collected from a small ridge on the lower slope of the southern Calabrian Ridge (Pisano Plateau, 36°15.250′ N,

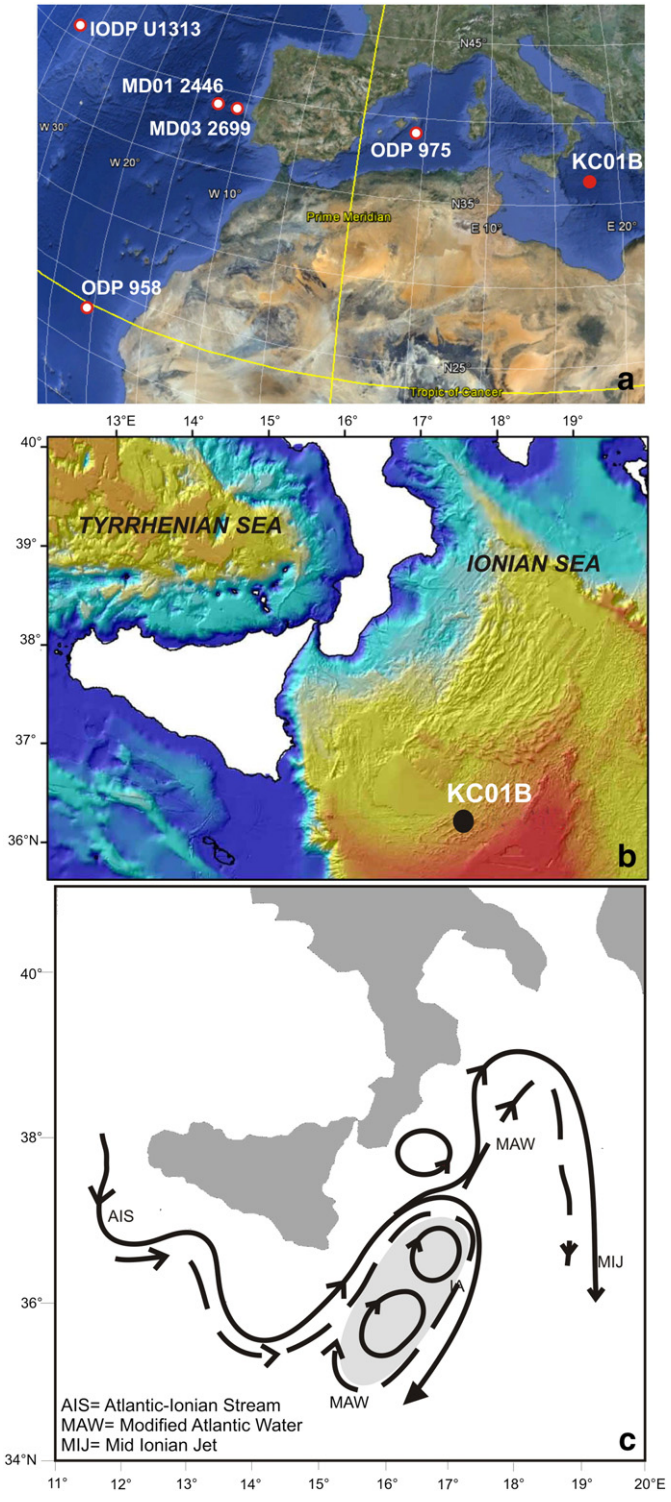

Fig. 1. (a) Location map of the investigated core site KC 01B and the discussed references cores; (b) bathymetric map of the Ionian Sea (DTM 450 m resolution retrieved from http://portal.emodnet-hydrography.eu/EmodnetPortal/index.jsf#); (c) mesoscale surface water circulation features of the Ionian Sea (from Napolitano et al., 2000 modified) are indicated (AIS = Atlantic-Ionian Stream, MAW = Modified Atlantic Water, MIJ = Mid Ionian Jet).

17°44.340′ E, 3643 m water depth; Fig. 1) during cruise MD69 of the R/V Marion Dufresne in 1991.

The lithology consists of hemipelagic marls, with intercalation of sapropels and the presence of a number of thin tephra layers and few thin turbidite levels (Castradori, 1993; Sanvoisin et al., 1993; Langereis et al., 1997; Lourens, 2004).

This 37 m thick sediment sequence represents an invaluable opportunity of investigating the early to late Pleistocene. Core KC01B has been intensively studied from different points of view, i.e., planktonic foraminifera, nannoplankton, stable isotopes, chemical and paleomagnetic analyses, tephra and sapropel presence (Castradori, 1993; Sanvoisin et al., 1993; Dekkers et al., 1994; Langereis et al., 1997; van Santvoort et al., 1997; Rossignol-Strick et al., 1998; Rossignol-Strick and Paterne, 1999; Lourens, 2004; Maiorano et al., 2013; Insinga et al., 2014).

Moreover, Core KC01B is well known in the chronostratigraphic literature because it was used for the construction of the Astronomical Time Scale (ATS) (Langereis et al., 1997) in the Mediterranean region and to propose the Tyrrhenian as a regional stage for the Upper Pleistocene (Cita Sironi et al., 2005). The ATS is based on the correlation of dominantly precession-controlled sedimentary cycles (i.e. sapropels and carbonate cycles) to astronomical parameters. In particular, this core was claimed to fill most of the gap between the oldest sapropel (S12) documented in marine sediments (piston core RC9-181—eastern Mediterranean Sea) dated at 483 ka (Lourens et al., 1996a) and the youngest sapropel (v) exposed in the land-based marine successions of the Vrica section (Southern Italy) dated at 1.280 Ma (Lourens et al., 1996b).

Concomitantly, Rossignol-Strick et al. (1998) proposed an alternative independent age model based on tuning of the oxygen isotope record of KC01B with the ice sheet model of Imbrie and Imbrie (1980).

Differences between both age models are in the order of 0–5 kyr and result from the choice of two different target curves and the adopted time lags between insolation forcing and climate response (Langereis et al., 1997) (for discussion see Hilgen et al., 1993; Lourens et al., 1996a). Largest differences (in the order of 10 kyr) between both age models occur around 618 and 785 ka.

Subsequently, Lourens (2004) established an improved sapropel-tuned age model for this core based on high-resolution colour reflectance correlation with the Ocean Drilling Project (ODP) Site 964. This time-scale resulted from a revised chronology of the marine isotope record of Rossignol-Strick et al. (1998), implying a much more uniform change in sedimentation rate for the Ionian Sea cores and a good fit with other Mediterranean and open ocean marine isotope records.

We studied the sediment interval through sections 21-16 of the core (between 21.82 and 15.85 m composite depth, spanning the time interval from 507.3 to 292.1 ka—Lourens, 2004). This interval includes three sapropels (S10, S11 and S12) (Lourens, 2004) (Fig. 2).

4. Methods

Quantitative micropaleontological analyses were performed on 596 samples with a spacing of 1 cm (average time resolution of ~380 yr). Samples were washed through 63 micron sieves and oven dried at 50 °C. Planktonic foraminiferal assemblage composition was determined analysing the >125 μm size fraction. For the micropaleontological census study, each sample was divided with a microsplitter to obtain unbiased aliquots with more than 300 planktonic foraminifers per sample. All taxa are quantified as percentages of the total number of planktonic foraminifers. The faunal data sets described in this paper have been archived, and are available in digital form, at PANGEA.

In this study, *Globigerinoides sacculifer* includes *Globigerinoides trilobus*, *G. sacculifer* and *Globigerinoides quadrilobatus* (sensu Hemleben et al., 1989); *Neogloboquadrina pachyderma* sinistral (sin) has been counted separately from the dextral (dex) form.

We distinguished *Neogloboquadrina incompta* from *N. pachyderma* by its development of a distinct apertural rim and a more lobulate outline. These taxa showed different vertical distribution and ecology. Studies performed on living planktonic foraminifers in Japan seas and in the eastern North Atlantic document the presence of *N. incompta* in

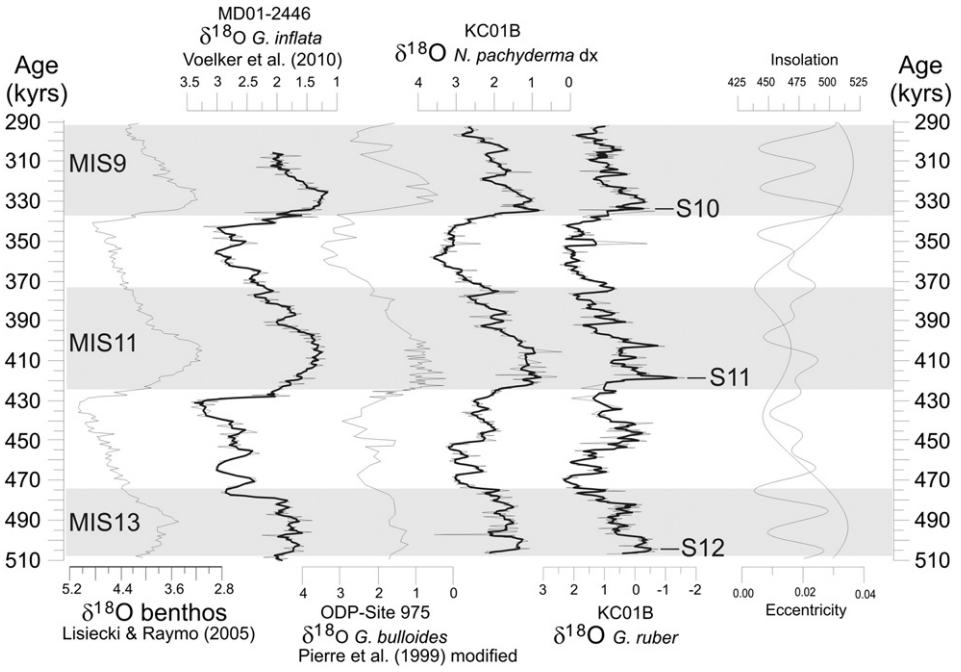

Fig. 2. Comparison in time domain between the benthic oxygen isotopic stack of Lisiecki and Raymo (2005), the δ18O *G. inflata* record of Voelker et al. (2010), the δ18O *G. bulloides* record of Pierre et al. (1999) modified by Lourens (2004) and Kandiano et al. (2012), the δ18O *Globigerinoides ruber* and *Neogloboquadrina pachyderma* dex records from the study KC01B core [3 points moving average (thick black curve) are superimposed on the δ18O raw data], and the astronomical insolation curve of Laskar et al. (2004).

shallower and warmer waters compared to *N. pachyderma* (Schiebel et al., 2001; Kuroyanagi and Kawahata, 2004).

Moreover, different morphotypes of *G. ruber* (white) were identified using the morphotype concept of Wang (2000). The typical *G. ruber* (d'Orbigny, 1839) is reported as *G. ruber* sensu stricto (s.s.), whereas *Globigerinoides elongatus* (d'Orbigny, 1826) and *Globigerinoides gomitulus* (Seguenza, 1880) are grouped and reported as *G. ruber* sensu lato (s.l.).

Several investigations, based on molecular genetics and geochemistry, highlighted the need to revise the taxonomy of *G. ruber* (d'Orbigny, 1839) which shows remarkable "morphological" variations (inter alias Darling et al., 1999; Kuroyanagi et al., 2008). In addition, the discrimination of the different morphotypes appears to be necessary because they have significantly different habitat preferences and thus different stable isotopic signals (Wang, 2000; Kuroyanagi and Kawahata, 2004; Kawahata, 2005; Loewemark et al., 2005; Lin and Hsieh, 2007; Numberger et al., 2009). On the other hand, the recent investigation in the Gulf of Mexico of Thirumalai et al. (2014) reports no evidence for discrepancies in s.s.-s.l. calcifying depth habitat or seasonality. The controversial outcomes reported suggest that additional studies on the relationship between living foraminiferal distribution and oceanographic conditions (productivity, stratification) in different basins are necessary to build a more extensive picture of the ecological requirements of different foraminiferal genetic types. In this work, we distinguished between different morphotypes in order to test if they presented different distribution patterns in the past.

The paleoclimate curve was calculated following Cita et al. (1977) and Sanvoisin et al. (1993). It represents the algebraic sum of warm-water species percentages (expressed as positive values) and cold-water species percentages (expressed as negative values) based on ecological preferences and modern habitat characteristics reported in Hemleben et al. (1989), Rohling et al. (1993), and Pujol and Vergnaud-Grazzini (1995). Warm water species are all *G. ruber* (white and pink varieties), *G. sacculifer*, *Globigerinoides tenellus*, *Globigerina rubescens*, *H. siphonifera* (including *Globigerinella calida*) and *Orbulina universa*. The cold water species are *G. bulloides*, *Globigerinita glutinata*, *Globorotalia scitula*, *Turbototalita quinqueloba* and *N. pachyderma* (dex). Negative and positive values of the curve allow qualitative estimates for cold and warm surface water respectively.

The paleoproductivity curve is based on a combination of planktonic foraminiferal species: it is calculated as the sum of *G. bulloides*, *G. glutinata* and *T. quinqueloba* percentages. All these taxa are related to high productivity environments (Bè and Tolderlund, 1971; Fairbanks and Wiebe, 1980; Pujol and Vergaud Grazzini, 1989).

In order to reconstruct paleoenvironmental and paleoceanographical conditions, the relative abundance of some species or groups considered in this study are plotted in percentages with respect to the total foraminiferal assemblage versus time. We assume that the habitat characteristics of the different species during the Pleistocene were similar to those observed today.

Stable isotope analyses were carried out on about 10–15 specimens of the planktonic foraminifers *N. pachyderma* (dex) and *G. ruber* (s.s. and s.l.) (from the >150 μm fraction) using an automated carbonate reaction device Kiel III coupled to a Thermo-Finnigan MAR253 Analytical precision was better than 0.03 and 0.05‰ for $\delta^{13}C$ and $\delta^{18}O$ respectively as deduced from international NBS-19, and in-house Naxos standards.

5. Age control

For the time interval considered in this work (290–510 ka), the age model by Lourens (2004) was partially modified and fine-tuned, considering the new chronological constraints on Pleistocene sapropel depositions (Konijnendijk et al., 2014).

We adopted the revised sapropel chronological framework in the eastern Mediterranean (ODP sites 967 and 968) provided by Konijnendijk et al. (2014) using the highly linear relation between the elemental ratio of titanium and aluminium in the sediment and insolation. The late Pleistocene sapropel chronology of Konijnendijk et al. (2014) presents deviation from Lourens (2004) down to ~400 ka, where sapropel S^b in ODP 967/968 (Emeis et al., 2000) is correlated to one insolation cycle older. Consequently, Sapropel S11 in KC01B [corresponding to sapropel S^b in ODP 967/968 (Konijnendijk et al., 2014)]

does not correspond to insolation cycle 38 (as reported in Lourens, 2004 at 407 ka) but to cycle 40 with a corresponding age of 418.9 ka (Konijnendijk et al., 2014).

As additional constraint, we used the tuning of the new high-resolution $\delta^{18}O$ data from *N. pachyderma* (sin) with the open-ocean benthic oxygen isotopic stack from Lisiecki and Raymo (2005) (Fig. 2).

Interpolation between consecutive tie-points was carried out by a linear function, assuming a constant sedimentation rate between the consecutive tie-points (mean sedimentation rate of 0.035 m/ka) and resulted in a higher resolution age control than in previous investigations (Castradori, 1993; Sanvoisin et al., 1993; Dekkers et al., 1994; Langereis et al., 1997; van Santvoort et al., 1997; Rossignol-Strick et al., 1998; Rossignol-Strick and Paterne, 1999). Data used for the age model construction are listed in Table 1.

This new Mediterranean $\delta^{18}O$ stack of *N. pachyderma* (dex) in the core KC01B has been compared with the $\delta^{18}O$ data of *G. inflata* of Voelker et al. (2010) from the Atlantic Ocean and with the $\delta^{18}O$ records of *G. bulloides* from ODP-site 975 studied by Pierre et al. (1999) and modified by Lourens (2004) and Kandiano et al. (2012). The good visual comparison between these climatic records supports the adopted age model (Fig. 2).

6. Results

6.1. Foraminiferal assemblages

Foraminiferal assemblages are rich and well preserved. The Shannon–Weaver Index commonly varies between 0.99 and 2.6 (Fig. **3**) and exhibits a sharply decreasing trend in diversity during the glacials MIS 12 and MIS 10. The more pronounced minima occur in the upper part of the glacial periods, when more than the 80% of the assemblages is composed by *T. quinqueloba*, neogloboquadrinids (*N. pachyderma* (dex) and *Neogloboquadrina dutertrei*) and *G. bulloides* (Fig. **3**). The remaining 20% of the assemblages is represented by *G. scitula* and *G. glutinata*. During the interglacials the diversity is higher with dominance of *G. ruber* group (about 50%) and the presence of other warm water taxa such as *O. universa*, *H. siphonifera*, *G.rubescens* and *G. tenellus* (10%). *G. bulloides*, neogloboquadrinids and *T. quinqueloba* show frequencies ranging from 10 to 20%.

The presence of *G. inflata* appears not to be related to glacial–interglacial phases; however higher abundances occur during interglacials (Fig. **3**).

A discontinuous pattern is observed in the distribution of *G. sacculifer* and *G. truncatulinoides*. *G. sacculifer* peaks during interglacial phases with a maximum value of about 20% (Fig. **3**). Its distribution is discontinuous during MIS 13, more continuous during MIS 11 and MIS 9. *G. truncatulinoides* characterizes the foraminiferal assemblages during the middle and upper part of interglacials. The maximum abundance of this taxon (20–25%) is recorded during MIS 11 (Fig. **3**).

7. Discussion

7.1. Glacials

Based on the planktonic foraminifera climatic curve, full glacial conditions occur during the upper part of MIS 12 and MIS 10 (Fig. 4). The climate conditions detected during the initial part of MIS 12 and MIS 10 are warmer than expected for a glacial stage as they fall in the range of values prevailing during the previously interglacials MIS 11 and MIS 9 (Fig. 4). These temperatures are principally related to higher percentages of warm surficial waters *G. ruber* group (Fig. 4). At this time, the assemblages are characterized by the dominance of *G. ruber* (s.l.) relative to *G. ruber* (s.s.). All these morphotypes occur in tropical-subtropical regions and prefer well-stratified waters but they show different habitats and seasonal preferences. In general, *G. ruber* (s.l.) calcifies deeper than *G. ruber* (s.s.) (Wang, 2000; Loewemark et al., 2005) and reflects different nutrient availability due to stratification of the water column (Lin et al., 2004). Based on the ecological divergence of the morphotypes, we interpret the higher relative abundance of *G. ruber* (s.l.) during the early part of MIS 12 and 10 as indicative primarily of the deepening of the summer thermocline. Probably *G. ruber* (s.l.) has shifted their habitat in order to avoid oligotrophic surface waters documented at this time by the low values of the productivity curve (Fig. 4). In the present Mediterranean Sea, low levels of production occur in summer, when the summer thermocline deepens to ~90 m leading to a stable stratification (Klein and Coste, 1984; Krom et al., 1992). The small differences between $\delta^{18}O$ of *N. pachyderma* and *G. ruber* show that the two taxa share a similar habitat indicating more homogenous conditions during this interval between surface and intermediate waters (Fig. 4).

The climatic conditions detected during early MIS 12 in core KC01B are coeval with the relative wintertime warmer sea surface temperatures (SST) documented in the nearshore waters off Portugal and in the western Mediterranean basin by Voelker et al. (2010) and associated with the increased heat transport by the Azores Current across the Atlantic. Moreover, the warming detected during the lower half of MIS 10 displays the same warm temperature anomaly in the SST record of Site 980 (North Atlantic, Feni Drift) (McManus et al., 1999) and site 1089 (South Atlantic Subtropical Front) (Cortese et al., 2007) during full glacial MIS 10 centred at ca. 350 ka and linked by the authors to a stronger than usual Agulhas Current influence. These similarities can be explained by the quick response of sub-surficial Mediterranean waters to atmospheric processes during both glacial stages. The warming occurring during the glacial half of both glacial MIS 10 and MIS 12 implies an extra-regional connection between the Mediterranean sea and the northern and southern hemisphere.

The subsequent increase in abundances of cold-water indicators *T. quinqueloba*, *N. pachyderma* (dex) and *G. bulloides* document the establishment of full glacial conditions during MIS 12 and MIS 10 at about 455 ka and 360 ka, respectively (Fig. 4). Well-known environmental preferences of these species for nutrient-rich environments (Bè and Tolderlund, 1971; Fairbanks and Wiebe, 1980; Reynolds and Thunell, 1986; Pujol and Vergnaud-Grazzini, 1995; Sierro et al., 2003) suggest productive sea surface waters as also supported by the highest values of the paleoproductivity curve (Fig. 4). At this time the fertilization can be triggered by the concurrence of different factors. One is represented by eolian input due to enhanced North-African dust deposition in the eastern Mediterranean (Roberts et al., 2011) during the upper part of the last five glacial stages. However, eolian dust in general does not seem to provide an adequate and/or continuous source of nutrients to enhance primary production (Krom et al., 2005; Incarbona et al., 2008). Another important factor may be the higher buoyancy gradient due to the reduced Atlantic surface-waters inflow that has altered the equilibrium of vertical mixing in the water column.

The glacial sea-level lowstand at the time of MIS 12 and MIS 10, leads to a reduced Atlantic surface-water influx and thus to shoaling of the density gradient (pycnocline) between intermediate and surface waters within the Mediterranean. This shoaling is similar to what has been suggested for other glacial sea-level lowstands (Rohling and Gieskes, 1989; Rohling, 1991, 1994; Myers et al., 1998). This factor is more evident during MIS12 when sea level was about 125 m below present (Rohling et al., 2009) (Fig. 4). MIS 12 is generally dominated by higher

Table 1
Tie-points used in this work for the construction of the age model.

Tie-point	Depth (mcd)	Age kyr	Reference
Sapropel S′	15.74	287.5	Konijnendijk et al. (2014)
Sapropel S10	16.84	332.3	Konijnendijk et al. (2014)
Base MIS 9	17.15	337	Lisiecki and Raymo (2005)
Sapropel S11	19.27	418.9	Konijnendijk et al. (2014)
Base MIS 12	20.83	474	Lisiecki and Raymo (2005)
Sapropel S12	21.74	504.5	Konijnendijk et al. (2014)

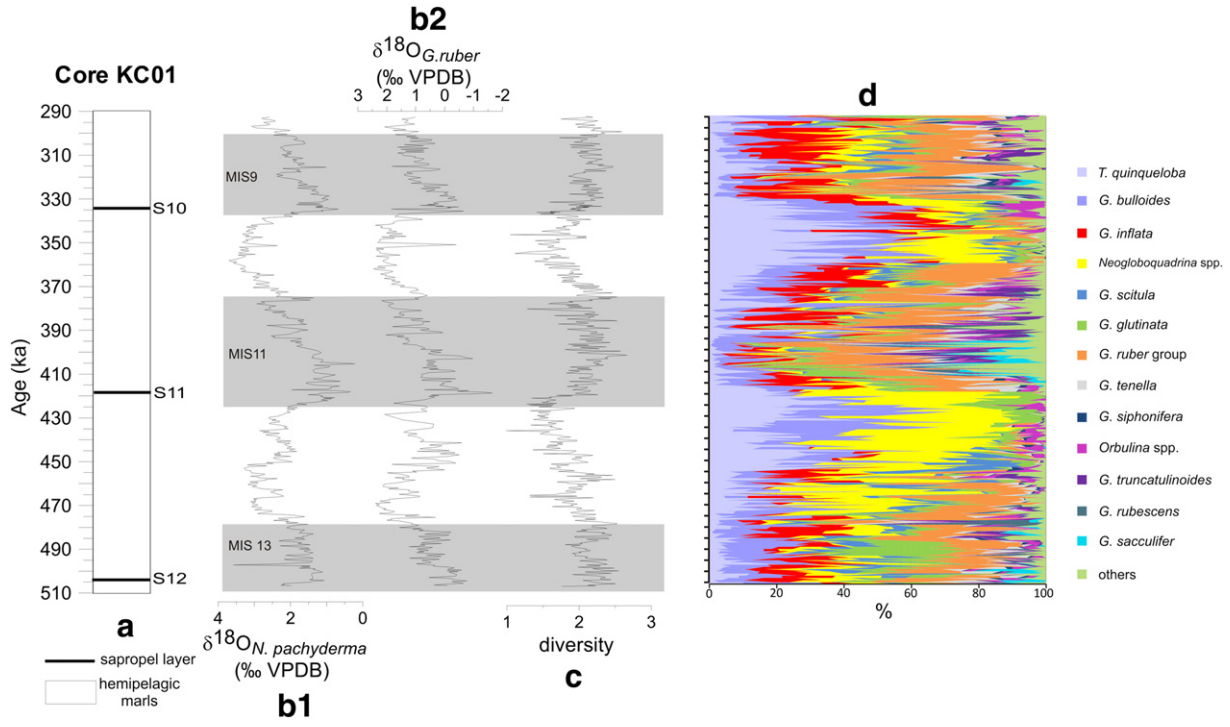

Fig. 3. (a) Lithological log of sedimentary investigated time interval of core KC 01B, (b) planktonic oxygen isotope records, (c) diversity and (d) foraminiferal distribution (in percentages of total assemblages versus age) of the identified species. As "other" we grouped taxa with percentages <0.5%. Chronology of sapropel (S10–S12) are according to Konijnendijk et al. (2014).

abundances (compared to MIS 10) of *N. pachyderma* (dex) and *N. dutertrei* reaching up to 60% of the total assemblage. These taxa are indicative for the intensity of the deep chlorophyll maximum (DCM), occurring when the upper part of the water column is isothermal and cold (Rohling and Gieskes, 1989; Pujol and Vergnaud Grazzini, 1995). Such DCM may develop during periods of reduced deep mixing. Similar evidence comes from the offset observed between *N. pachyderma* and *G. ruber* oxygen isotope values (Fig. 4) that document stratification between the surficial and the lower part of the photic zone. This is consistent with a different density gradient in the water column due to the large decrease in Atlantic surface inflow.

The colder intervals of the investigated glacials are characterized by peaks in abundance of *N. pachyderma* (sin) (with values of 18%) at times of extremely negative, cold values of the climate curve (Fig. 5). *N. pachyderma* (sin) is known not only to prefer polar-subpolar waters (Bé and Tolderlund, 1971; Reynolds and Thunell, 1986; Hemleben et al., 1989; Dieckmann et al., 1991; Johannessen et al., 1994), but also to be the dominant planktonic foraminiferal species during Heinrich events recorded in the North Atlantic Ocean (Heinrich, 1988; Bond et al., 1992).

Very rare specimens of *N. pachyderma* (sin) have been towed at the end of summer in the Ionian Sea (Pujol and Vergnaud-Grazzini, 1995); however this taxon is generally uncommon (<5%) in the Mediterranean during the Quaternary (Thunell, 1978; Rohling and Gieskes, 1989; Rohling et al., 1993; Hayes et al., 1999, 2005; Sprovieri et al., 2003, 2012; Triantaphyllou et al., 2009; Siani et al., 2010). Significant percentages of *N. pachyderma* (sin) in the western Mediterranean Sea during the last glacial period have been interpreted as the result of polar water intrusions into the Mediterranean via the Strait of Gibraltar at the time of the Atlantic Heinrich events (Cacho et al., 1999;

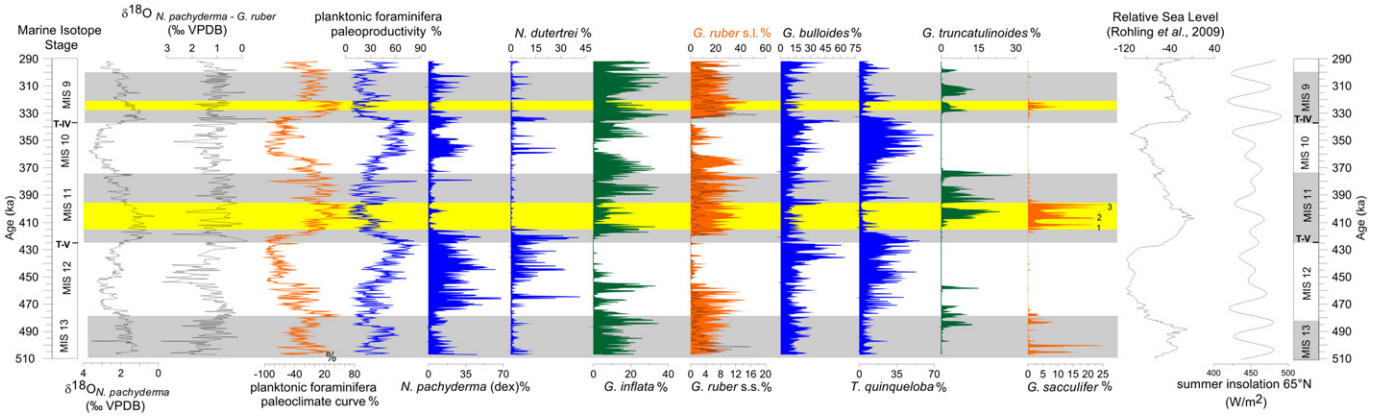

Fig. 4. Quantitative distribution patterns of selected planktonic species (percentage values plotted versus age) during MIS 13 and MIS 9 from core KC01B. Curve of Summer insolation at 65°N is from Laskar et al. (2004). Relative sea level record is from Rohling et al. (2009). Grey bands indicate interglacial intervals according to oxygen isotope chronology of Lisiecki and Raymo (2005); yellow bands correspond to the climatic optimum intervals. The MIS 13–9 and Termination V (T-V) and IV (T-IV) are indicated.

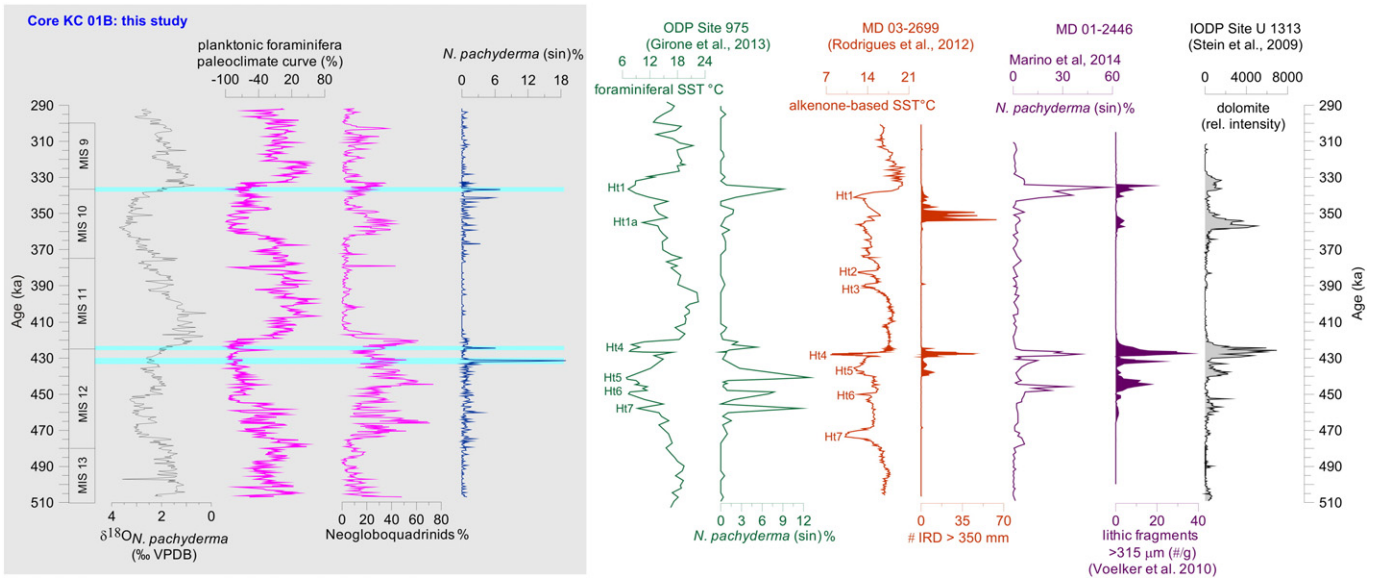

Fig. 5. Comparison between *N. pachyderma* (dex) δ18O, foraminiferal paleoclimate curve; neogloboquadrinids and relative abundance of *N. pachyderma* (sin) records at core site KC01B and foraminiferal SST (f) and plot of *N. pachyderma* (sin.) at Mediterranean ODP Site 975 (Girone et al., 2013b). For the Atlantic climate records are indicated: Alkenone-based SST and relative proportion of ice ice-rafted detritus (IRD) at Core MD03-2699 (Rodrigues et al., 2011). *N. pachyderma* (sin) distribution record and (m) proportion of IRD at core MD 01-2446 (Voelker et al., 2010 and Marino et al., 2014, the dolomite relative intensity at IODP Site U1313 (Stein et al., 2009). Light blue bands mark abrupt fluctuations of *N. pachyderma* (sin.) correlated to Heinrich-type events recorded at the western Mediterranean and Atlantic sites.

Pérez-Folgado et al., 2003; Sierro et al., 2005). The increases in the relative abundance of *N. pachyderma* (sin), coeval with a SST drop comparable for distribution and amplitude to the Heinrich-type events, have also been documented during MIS5 (Combourieu Neobout et al., 2002; Martrat et al., 2004), throughout MIS 15–9 (Girone et al., 2013a) and during MIS 100 (Becker et al., 2006) in the western and eastern basin.

At the investigated site (Fig. 5), we observe that the distribution of *N. pachyderma* (sin) is positively correlated with that of neogloboquadrinids and that, despite the different time-resolution of the data, the significant increase in abundance of *N. pachyderma* (sin) correlates well with that observed in the western Mediterranean (ODP Site 975) (Girone et al., 2013b) and North Atlantic Heinrich-type events (Stein et al., 2009; Rodrigues et al., 2011). In the Mediterranean Sea high abundances of neogloboquadrinids are often associated with low-density water masses as observed in sapropel deposition during colder climatic phases (Capotondi and Vigliotti, 1999; Negri et al., 1999; Stefanelli et al., 2005). We can speculate that the cooling of Atlantic inflowing waters due to iceberg melting, already documented in the western Mediterranean (Sierro et al., 2005; Frigola et al., 2008), could also have affected the hydrological setting of the Ionian Sea. On the other hand, this may have occurred because of the intense freshwater discharges into the Mediterranean through the Black Sea from meltwater of lakes dammed by the Scandinavian ice sheet (Sprovieri et al., 2012) and/or from NW African (Atlas) mountain glaciers (Rogerson et al., 2008). At present, we do not have clear evidence for local sources of water; further high-resolution studies are necessary to understand the occurrence and distribution of *N. pachyderma* (sin) in the Mediterranean Sea.

7.2. Interglacials

From the paleoclimatic curve typical full interglacial conditions can for the first time be recognized during MIS 11 at ~420 ka. The warm conditions culminate between 415 and 395 ka when the microfauna is characterized by the presence of tropical-subtropical species *G. sacculifer* that prefers warmer and shallower waters than *G. ruber* (Kuroyanagi and Kawahata, 2004). At present, this species lives in the western Mediterranean at the end of summer (Pujol and Vergnaud-Grazzini, 1995) and its distribution in surface sediments from west to east reflects its strong temperature dependence (Thunell, 1978). The increase in abundance of *G. sacculifer* in the Mediterranean has been reported to be associated to "Climatic Optima" during the late Holocene intervals e.g. Medieval Warm Period, the Roman Age, the late Bronze Age and the Copper Age (Piva et al., 2008; Lirer et al., 2013, 2014). According, we interpret the occurrence of this species in core KC01B during interglacial MIS 11 and MIS 9 as indicative of the "Climatic Optimum interval/Thermal maximum". This interpretation concurs with the paleoclimate reconstruction of the same period and for the same core, based on calcareous nannofossil assemblages (Maiorano et al., 2013). The presence of an extended "Climatic Optimum", lasting ~30 ka, has been documented in SST records across the world ocean (McManus et al., 1999; Hodell et al., 2000; De Abreu et al., 2005; Kandiano and Bauch, 2007; Dickson et al., 2009; Stein et al., 2009; Voelker et al., 2010), from Antarctic ice cores (Petit et al., 1999; Jouzel et al., 2007) and in terrestrial pollen records (Tzedakis, 2010). It occurs after a prolonged deglacial warming (Termination V) that extends into MIS 11 with global and regional climate variability (Milker et al., 2013 and references therein).

The present high-resolution database provides new climatostratigraphic insights for the "Climatic Optimum" of the central Mediterranean region. It is interesting to note that, during MIS 11, *G. sacculifer* shows three different peaks of abundance concomitant with the decrease/absence of *G. truncatulinoides* (Fig. 4). *G. sacculifer* reaches its maximum quantity in the Eastern Basin, where surface waters remain relatively warm, and low nutrient contents prevail throughout the year due to the a relatively stable pycnocline at depth (Pujol and Vergnaud Grazzini, 1995).

Higher values of living *G. truncatulinoides* have been observed in the Mediterranean in areas of intense water mixing during winter, i.e. the North Western Basin (Pujol and Vergnaud Grazzini, 1995), while in the more stratified waters of the Eastern Basin it is rarely found (Core top database of Kallel et al. (1997)).

Distributional trends of these taxa document that the "Climatic Optimum" of MIS 11 was not uniform but characterized by three distinct intervals with a year-around water column stratification and/or a weaker winter mixing with a consequent limited food supply. At the

same time, higher values of the paleoclimate curve imply warmer superficial conditions or elevated winter sea surface temperatures (i.e. increase of the warm water taxa). The three warmer intervals present an estimated age of 415–410 ka, 408–403 ka, and 400–395 ka, respectively.

An interesting remark is that the peak from 400 to 395 ka is coeval with and shows the same length of the warm interval (400–395 ka Fig. 4) recorded in marine paleoclimate data off Iberia at the end of the MIS 11c (Koutsodendris et al., 2014). Since that interval corresponds to an insolation minimum, this implies that orbital insolation forcing is not the warming cause.

Koutsodendris et al. (2014) motivate the North-Atlantic warmth as an interhemispheric teleconnection between strong leakage in the South Atlantic and Atlantic Meridional Overturning Circulation (AMOC)-driven warmth in the North Atlantic maintaining temperate conditions off Iberia and the continental Europe during the MIS11c. Accordingly, we speculate that the warmer intervals identified in our record are the result of an ocean-climate teleconnection between the high- and low-latitudes. Nevertheless additional sites are necessary in order to understand the exact mechanisms and extent of such climatic variability at time of the "Climatic Optimum".

The observed post-glacial temperature increase after Termination V does not match the Holocene SST trend when the "Climatic Optimum" already began after Termination I coincident with Sapropel S_1 deposition (Capotondi et al., 1999; Rohling and De Rijk, 1999; Cacho et al., 2001; Triantaphyllou et al., 2009). However a direct comparison between MIS 11 and MIS 1 is difficult to make because of a different phase in the orbital parameters. In fact, the present interglacial (Holocene) spans a single summer insolation maximum (summer at 65°N), while MIS 11 interglacial optimum spans two (weak) insolation maxima (Laskar et al., 2004).

From 392 ka onward, the MIS11 in core KC01B is characterized by oligotrophic surface waters during summer (Fig. 4) and eutrophic during winter, when deep-water masses are well-ventilated, as testified by the presence of *G. inflata* and *G. truncatulinoides*. These conditions are comparable to those in the present-day Ionian Sea. At present, *G. inflata* and *G. truncatulinoides* dominate the fauna of the winter assemblages in the Ionian Sea (Pujol and Verganud Grazzini, 1995). Distribution of planktonic foraminifera during MIS 9 document similar general trends as described for MIS 11, with a thermal maximum between 326 and 320 ka (Fig. 4). However, MIS9 is characterized by lower percentages of warm-water taxa compared to MIS 11, thus suggesting that SSTs were lower during MIS9 than during MIS11.

7.3. Sea surface changes during transition T-V and T-IV

Termination V in core KC01B is marked by a decrease of $\delta^{18}O$ of *N. pachyderma* from +2.5‰ at 430 ka to +0.8‰ at 420 ka (Fig. 6). During this transition the planktonic foraminifera content shows significant changes related to different environmental conditions (Fig. 6) and provides new data on how the transitions evolved from glacial to interglacial.

The high abundance of the herbivorous species *G. bulloides* and *T. quinqueloba* from ~430 to ~425 ka (Fig. 6) suggests enhanced nutrient supply in the sub-surface water masses. As these species reach the highest concentrations in upwelling regions or in areas of vigorous vertical mixing in the water column (Reynolds and Thunell, 1986), where high phytoplankton productivity prevails, we can hypothesize the presence of an upwelling regime or continental coastal input at this time, probably induced by the presence or intensification of the gyre similar to the one observed at present in the Ionian Sea (Civitarese et al., 2010; Gačić et al., 2010). The absence of *G. inflata* (Fig. 4) supports this oceanographic scenario, as this species prefers temperate and high nutrient waters not affected by upwelling processes (Giraudeau, 1993). The increase in primary productivity is also documented by the calcareous nannofossil data (Maiorano et al., 2013). This phase is coeval with a peak of iron-rich terrigenous dust at ODP Site 958 (Helmke et al., 2008), related to the strengthening of trade winds over northwestern Africa. Probably, this strengthening of westerlies is also associated with the strengthening of the Atlantic Ionian Stream jet leading to a dynamic activity of mesoscale features such as meanders and eddies. The latter results in mixing thus in enhanced nutrient supply, and leads to increased primary production. Several oceanographic studies performed in different areas of the Mediterranean document that variability in mesoscale hydrographic features leads to an increase of biological productivity (Estrada, 1996; Christaki et al., 2011).

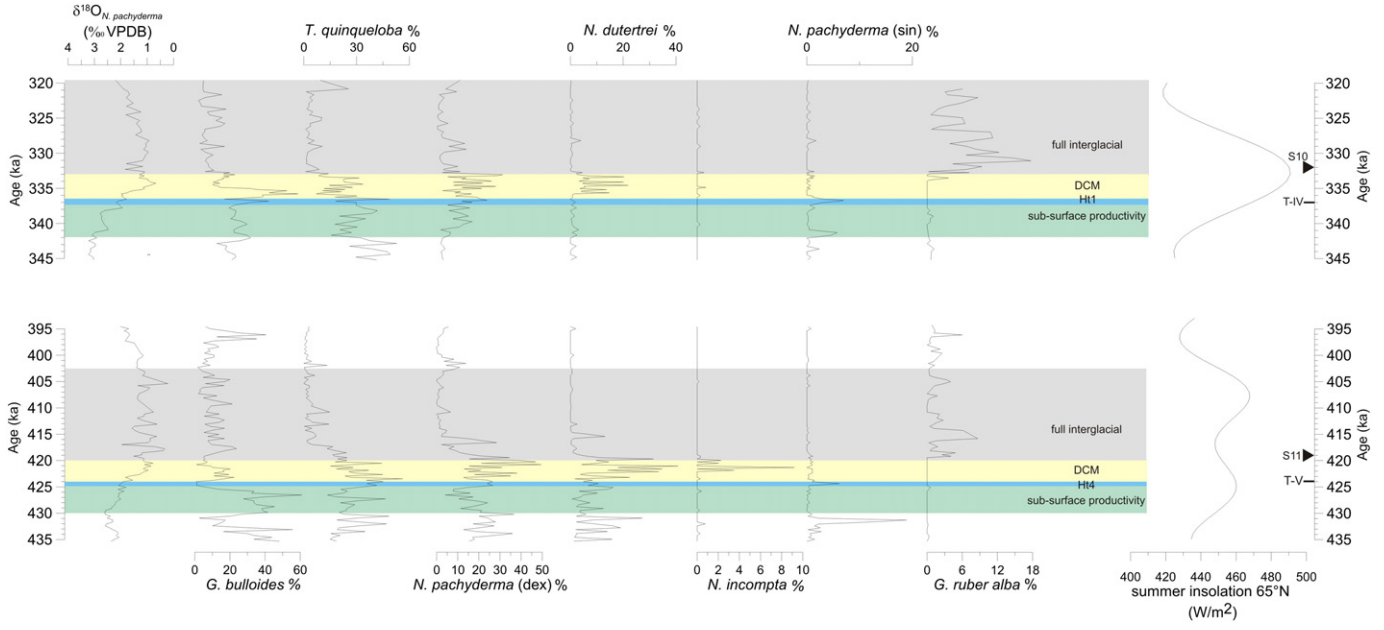

Fig. 6. Down core distribution of selected planktonic species during Termination V and IV from core KC01B. Curve of Summer insolation at 65°N is from Laskar et al. (2004). The colour bands indicate the different phases (see text for the descriptions). Position of sapropel S10 and S11 and Termination V (T-V) and IV (T-IV) are indicated. H1 and H4 refer to Heinrich-like event 1 and 4 following the nomenclature adopted by Girone et al. (2013b).

The relatively low abundance of *G. bulloides* between 424 and 420 ka, together with the increasing percentages of *N. pachyderma* (dex) and *N. dutertrei* (Fig. 6) documents the transition to stratified water conditions and the development of a DCM. The co-occurrence of *N. incompta*, a species that prefers shallower and warmer waters than *N. pachyderma* (Kuroyanagi and Kawahata, 2004), also suggests amelioration of climate (Fig. 6).

We interpret this microfaunal assemblage as the result of freshwater input/land-derived nutrients associated with the climatic transition from glacial conditions of MIS 12 to the interglacial conditions of MIS 11. Further evidence is provided by the steadily decreasing $\delta^{18}O$ of *N. pachyderma* during the same period (Fig. 6), which might be explained by a SST increase or a salinity decrease due to surface water freshening during this phase.

The increase in *G. ruber* abundance at around 420 ka together with lighter oxygen isotopic values in *N. pachyderma* reflects the influence of the African humid phase in the Ionian sea that culminates with sapropel layer S11 deposition at 418.9 ka (Konijnendijk et al., 2014) (Fig. 6).

This is suggested by the timing that is coherent with the onset of the wet phase over North-West Africa (Helmke et al., 2008), when the enhanced influence of the West African Monsoon system on the Saharan–Sahel region led to higher fresh-water input into the Mediterranean. During the early MIS 11 the African monsoon system intensification is also documented in marine records from the North Atlantic and western Mediterranean Sea and it has been related to the northward-moving of the Intertropical Convergence Zone (ITCZ) (Kandiano et al., 2012).

In general, changes in the planktonic foraminiferal distribution observed during transition T-IV lead to a similar climatic reconstruction as outlined for T-V (Fig. 6). The dominance of *G. bulloides* and *T. quinqueloba* from 342 to 337 ka points to enhanced nutrient content and mixing/upwelling during the first part of the transition from MIS 10 to MIS9. The subsequent replacement (~336–333 ka) of *N. pachyderma* and *N. dutertrei* suggests stratified conditions with a shallow mixed layer. Then, Sapropel S10 occurs at 332 ka (Konijnendijk et al., 2014) (Fig. 6).

Based on our data, the dynamics of the sea surface property during Termination V are due to the deglaciation and wind system variability. The timing and modalities of climate dynamics during the Terminations in different regions are as yet not fully understood. Recent investigations focus on the relative position of the Heinrich cold events that characterize all last five Terminations at a global scale (Cortese et al., 2007; Cheng et al., 2009; Barker et al., 2011; Marino et al., 2015). During the most recent Terminations I (MIS 2/MIS 1) and II (MIS 6/MIS 5) their positions show strong differences in these two deglaciations and point to a bipolar seesaw control mechanism for Termination II (Marino et al., 2015).

Observing the distributional trend of *N. pachyderma* (sin) in core KC01B, a "Heinrich-like" cold event (see paragraph above) is clearly detected within both the transitions T-V and T-IV (Fig. 6) in correspondence with a small drop in the oxygen isotope record (Fig. 6). Based on paleoceanographic inferences provided by planktonic foraminifera, these cold episodes occur approximately in the mid-point of the deglaciations, coincident with the increase in trade wind intensity off NW Africa (Fig. 6). This suggests that they are probably linked to the wind influence and thus to atmospheric conditions. This interpretation is also consistent with reported results from other ocean basins, indicating that Heinrich-like events are associated with stronger winds (e.g. Wang et al., 2001; Moreno et al., 2002; Itambi et al., 2009; Roberts et al., 2011). These are probably induced by southward shifts of the Inter Tropical Convergence Zone (Jullien at al., 2007). Accordingly, we conclude that the T-V and T-IV observed in the Mediterranean are not only regional events but are associated with a dynamic reorganization of global atmospheric conditions.

Our environmental scenarios are consistent with the sequence of major events documented in the last four Terminations that link the displacements of the ITCZ, the AMOC and the North Atlantic cooling (Cheng et al., 2009; Schneider et al., 2014; Marino et al., 2015).

During glacial–interglacial transitions T-IV and T-V the climate/ocean interaction was probably related to strong feedback processes: the weakening or shutdown of the AMOC due to enhanced freshwater input to the North Atlantic resulted in an increase in sea surface temperature within the tropics as well as in cooling of the North Atlantic and in the geographical shift of the wind system over North Africa.

Clearly, more data with good age control are needed from a wider area so to substantiate and evaluate extent and intensity of these events. This is not only needed to better understand mechanisms of paleoclimate change but is also relevant for our abilities to forecast potential future climate change processes.

8. Conclusions

A detailed study on planktonic foraminiferal assemblages from sediment core (KC01B) collected in the Ionian Basin (central Mediterranean Sea) allowed us to reconstruct the climate variability during glacial–interglacial periods between 500 and 300 ka (MIS 13–MIS 9). The main results can be summarized as follows:

- The early part of MIS 12 and MIS 10 is characterized by relatively "warm conditions" with a deepening of the summer thermocline derived from the quantitative distribution of *G. ruber* s.l. with respect to *G. ruber* s.s. Glacial conditions and eutrophic regimes are established in the upper half of the interval evidenced by significant increase of *T. quinqueloba*, *N. pachyderma* (dex) and *G. bulloides*. The colder intervals are interrupted by peaks in abundance of *N. pachyderma* (sin) coeval with north-Atlantic Heinrich-type cold events suggesting the close association of Central Mediterranean climate and North-Atlantic millennial-scale climate instability.
- Interglacials MIS 11 and MIS 9 have a prolonged "Climatic Optimum" lasting ~20 and 6 Ka respectively, as documented by the increase of the warm species *G. sacculifer*. Here for the first time we document that the extended warmth during the MIS 11c is characterized by three intervals with elevated winter sea surface temperatures and a weaker winter mixing.
- Complex paleoceanographic changes occurred during the glacial–interglacial transitions (T-V and T-IV) consistent with the sequence of major events documented in the last four Terminations that link the displacements of the ITCZ, the AMOC and the North Atlantic cooling.

The high-resolution investigations allow us to provide the timing of these changes occurring in the Mediterranean region and to link these to global climate events.

Acknowledgements

The authors acknowledge L. van Roij, A. Filippidi, and A. van Dijk for isotope measurements. Special thanks go to two anonymous reviewers and the editor Paul Hesse for their helpful comments and suggestions. Discussions with E. Bonatti, L. Vigliotti and P. Montagna are gratefully acknowledged. This study was financially supported by NWO (PASSAP, PASS), EU-Mast (Paleoflux), SISTEMA- PONa3_00369, NEXTDATA (PNR 2011-2013) and RITMARE (PNR 2012-2016)projects. This is contribution number 1873 of the CNR-ISMAR of Bologna.

References

Allen, J.I., Somerfield, P.J., Siddorn, J., 2002. Primary and bacterial production in the Mediterranean Sea: a modelling study. J. Mar. Syst. 33–34, 473–495.

Antoine, D., Morel, A., André, J.M., 1995. Algal pigment distribution and primary production in the Eastern Mediterranean as derived from Coastal Zone Color Scanner observations. J. Geophys. Res. 100, 16193–16209.

Barker, S., Knorr, G., Edwards, R.L., Parrenin, F., Putnam, A.E., Skinner, L.C., Wolff, E., Ziegler, M., 2011. 800,000 years of abrupt climate variability. Science 347, 0–5.

Bauch, H.A., Erlenkeuser, H., Helmke, J.P., Struck, U., 2000. A paleoclimatic evaluation of marine oxygen isotope stage 11 in the high-northern Atlantic (Nordic seas). Glob. Planet. Chang. 24, 27–39.

Bè, A.W.H., Tolderlund, D.S., 1971. Distribution and ecology of living planktonic foraminifera in surface waters of the Atlantic and Indian Oceans. In: Funnel, B.M., Riedel, W.R. (Eds.), The Micropaleontology of Oceans. Cambridge University Press, Cambridge, pp. 105–149.
Becker, J.F., Lourens, L.J., Raymo, M.E., 2006. High-frequency climate linkages between the North Atlantic and the Mediterranean during marine oxygen isotope stage 100 (MIS100). Paleoceanography 21. http://dx.doi.org/10.1029/2005PA001168 (PA3002).
Béthoux, J.P., 1979. Budgets of the Mediterranean Sea. Their dependence on the local climate and on the characteristics of the Atlantic waters. Oceanol. Acta 2, 157–163.
Béthoux, J.P., Morin, P., Madec, C., Gentili, B., 1992. Phosphorus and nitrogen behaviour in the Mediterranean Sea. Deep-Sea Res. 39, 1641–1654.
Béthoux, J.P., Gentili, B., Morin, P., Nicolas, E., Pierre, C., Ruiz-Pino, D., 1999. The Mediterranean Sea: a miniature ocean for climatic and environmental studies and a key for the climatic functioning of the North Atlantic. Prog. Oceanogr. 44, 131–146.
Bond, G., Heinrich, H., Broecker, W., Labeyrie, L., McManus, J., Andrews, J., Huon, S., Jantschik, R., Clasen, S., Simet, C., Tedesco, K., Klas, M., Bonani, G., Ivy, S., 1992. Evidence for massive discharges of icebergs into the North Atlantic Ocean during the last glacial period. Nature 360, 245–249.
Borghini, M., Bryden, H., Schroeder, K., Sparnocchia, S., Vetrano, A., 2014. The Mediterranean is becoming saltier. Ocean Sci. 10, 693–700.
Bosc, E., Bricaud, A., Antoine, D., 2004. Seasonal and interannual variability in algal biomass and primary production in the Mediterranean Sea, as derived from 4 years of SeaWiFS observations. Glob. Biogeochem. Cycles 18, GB1005.
Cacho, I., Grimalt, J., Pelejero, C., Canals, M., Sierro, F.J., Flores, J.A., Shackleton, N., 1999. Dansgaard–Oeschger and Heinrich event imprints in Alboran Sea paleotemperatures. Paleoceanography 14 (6), 698–705.
Cacho, I., Grimalt, J.O., Canals, M., Sbaffi, L., Shackleton, N.J., Schönfeld, J., Zahn, R., 2001. Variability of the western Mediterranean Sea surface temperatures during the last 25,000 years and its connection with the northern hemisphere climatic changes. Paleoceanography 16, 40–52.
Capotondi, L., Vigliotti, L., 1999. Magnetic and microfaunistical characterization of late Quaternary sediments in the Western Mediterranean (ODP Leg 161). Inference on sapropel formation and paleoceanographic evolution. In: Zahn, R., Comas, M.C., Klaus, A. (Eds.), Proceedings of the Ocean Drilling Program, Scientific Results, College Station TX, 161, 505-518.
Capotondi, L., Borsetti, A.M., Morigi, C., 1999. Foraminiferal ecozones, a high resolution proxy for the late Quaternary biochronology in the central Mediterranean Sea. Mar. Geol. 153, 253–274.
Castellari, S., Pinardi, N., Leaman, K., 2000. Simulation of water mass formation processes in the Mediterranean Sea: influence of the time frequency of the atmospheric forcing. J. Geophys. Res. 105, 24157–24181.
Castradori, D., 1993. Calcareous nannofossils and the origin of eastern Mediterranean sapropels. Paleoceanography 8, 459–471.
Cheng, H., Edwards, R.L., Broecker, W.S., Denton, G.H., Kong, X., Wang, Y., Zhang, R., Wang, X., 2009. Ice age terminations. Science 326, 248–252.
Christaki, U., Van Wambeke, F., Lefevre, D., Lagaria, A., Prieur, L., Pujo-Pay, M., Grattepanche, J.-D., Colombet, J., Psarra, S., Dolan, J.R., Sime-Ngando, T., Conan, P., Weinbauer, M.G., Moutin, T., 2011. The impact of anticyclonic mesoscale structures on microbial food webs in the Mediterranean Sea. Biogeosci. Discuss. 8, 185–220.
Cita Sironi, M.B., Capotondi, L., Asioli, A., 2005. The Tyrrhenian stage in the Mediterranean: definition, usage and recognition in the deep-sea record. Rendiconti Accademia Lincei 9 (16), 297–310.
Cita, M.B., Vergnaud-Grazzini, C., Robert, C., Chamley, H., Ciaranfi, N., D' Onofrio, S., 1977. Paleoclimatic record of a long deep-sea core from the eastern Mediterranean. Quat. Res. 8, 205–235.
Civitarese, G., Gačić, M., Lipizer, M., Eusebi Borzelli, G.L., 2010. On the impact of the Bimodal Oscillating System (BiOS) on the biogeochemistry and biology of the Adriatic and Ionian Seas (Eastern Mediterranean). Biogeosciences 7, 3987–3997.
Combourieu Nebout, N., Turon, J.L., Zahn, R., Capotondi, L., Londeix, L., Pahnke, K., 2002. Enhanced aridity and atmospheric high-pressure stability over the western Mediterranean during the North Atlantic cold events of the past 50 ky. Geology 30, 863–866.
Cortese, G., Abelmann, A., Gersonde, R., 2007. The last five glacial–interglacial transitions: a high-resolution 450,000-year record from the subantarctic Atlantic. Paleoceanography 22 (4), PA4203.
Crispi, G., Crise, A., Mauri, E., 1999. A seasonal three-dimensional study of the nitrogen cycle in the Mediterranean Sea: part II. Verification of the energy constrained trophic model. J. Mar. Syst. 20, 357–380.
d'Orbigny, A.D., 1826. Tableau méthodique de la classe de céphalopodes. Annales Des Sciences Naturelles, Paris France Ser. I 7, 1–277.
d'Orbigny, A.D., 1839. Mollusques, echinodermes, foraminiferes et polypiers, recueillis aux illes Canaries par Mm. Webb et Berthelot et décrits par Alcide D'Orbigny (2éme partie: Mollusques) (Paris: 117 pp.; 8 pls).
D'Ortenzio, F., Ribera d'Alcalà, M., 2009. On the trophic regimes of the Mediterranean Sea: a satellite analysis. Biogeosciences 6, 139–148.
Darling, K.F., Wade, C.M., Kroon, D., Leigh Brown, A.J., Bijma, J., 1999. The diversity and distribution of modern planktic foraminiferal small subunit ribosomal RNA genotypes and their potential as tracers of present and past ocean circulations. Paleoceanography 14, 3–12.
De Abreu, L., Abrantes, F., Shackleton, N., Tzedakis, P.C., McManus, J.F., Oppo, D.W., Hall, M.A., 2005. Ocean climate variability in the eastern North Atlantic during interglacial marine isotope stage 11: a partial analogue for the Holocene? Paleoceanography 20, PA3009. http://dx.doi.org/10.1029/2004PA001091.
Dekkers, M.J., Langereis, C.G., Vriend, S.P., Van Santvoort, P.J.M., De Lange, G.J., 1994. Fuzzy c-means cluster analysis of early diagenetic effects on natural remanent magnetisation acquisition in a 1.1 Myr piston core from the central Mediterranean. Phys. Earth Planet. Inter. 85, 155–171.
Dickson, A.J., Beer, C.J., Dempsey, C., Maslin, M.A., Bendle, J.A., McClymont, E.L., Pancost, R.D., 2009. Oceanic forcing of the Marine Isotope Stage 11 interglacial. Nat. Geosci. 2, 428–433.
Dieckmann, G.S., Spindler, S., Lange, M.A., Ackley, S.F., Eicken, H., 1991. Antarctic sea ice: a habitat for the foraminifer *Neogloboquadrina pachyderma*. J. Foraminifer. Res. 21, 181–194.
Emeis, K.C., Struck, U., Schulz, H.M., Rosenberg, M., Bernasconi, S.M., Erlenkeuser, H., Sakamoto, T., Martinez-Ruiz, F.C., 2000. Temperature and salinity variations of Mediterranean Sea surface water over the last 16,000 years from records of planktonic stable oxygen isotopes and alkenone unsaturation ratios. Palaeogeogr. Palaeoclimatol. Palaeoecol. 158 (3-4), 259–280.
EPICA community members, 2004. Eight glacial cycles from an Antarctic ice core. Nature 429 (6992), 623–628.
Estrada, M., 1996. Primary production in the northwestern Mediterranean. Sci. Mar. 60 (Suppl. 2), 55–64.
Fairbanks, R.G., Wiebe, P.H., 1980. Foraminifera and chlorophyll maximum: vertical distribution, seasonal succession, and paleoceanographic significance. Science 209, 1524–1526.
Frigola, J., Moreno, A., Cacho, I., Canals, M., Sierro, F.J., Flores, J.A., Grimalt, J.O., 2008. Evidence of abrupt changes in Western Mediterranean Deep Water circulation during the last 50 kyr: a high-resolution marine record from the Balearic Sea. Quat. Int. 181, 88–104.
Gačić, M., Borzelli, G.L.E., Civitarese, G., Cardin, V., Yari, S., 2010. Can internal processes sustain reversals of the ocean upper circulation? The Ionian Sea example. Geophys. Res. Lett. 37 (9), 1–5.
Giraudeau, J., 1993. Planktonic foraminiferal assemblages in surface sediments from the southwest African margin. Mar. Geol. 110, 47–62.
Girone, A., Capotondi, L., Ciaranfi, N., Di Leo, P., Lirer, F., Maiorano, P., Marino, M., Pelosi, N., Pulice, I., 2013a. Paleoenvironmental changes at the lower Pleistocene Montalbano Jonico section (southern Italy): global versus regional signals. Palaeogeogr. Palaeoclimatol. Palaeoecol. 371, 62–79.
Girone, A., Maiorano, P., Marino, M., Kucera, M., 2013b. Calcareous plankton response to orbital and millennial-scale climate changes across the Middle Pleistocene in the western Mediterranean. Palaeogeogr. Palaeoclimatol. Palaeoecol. 392, 105–116.
Hayes, A., Rohling, E.J., De Rijk, S., Kroon, D., Zachariasse, W.J., 1999. Mediterranean planktonic foraminiferal faunas during the last glacial cycle. Mar. Geol. 153, 239–252.
Hayes, A., Kucera, M., Kallel, N., Sbaffi, L., Rohling, E.J., 2005. Glacial Mediterranean sea surface temperature based on planktonic foraminiferal assemblages. Quat. Sci. Rev. 24, 999–1016.
Heinrich, H., 1988. Origin and consequences of cyclic ice rafting in the northeast Atlantic Ocean during the past 130,000 years. Quat. Res. 29, 142–152.
Helmke, J.P., Bauch, H.A., 2003. Comparison of conditions between the polar and subpolar North Atlantic region over the last five climate cycles. Paleoceanography 18 (2), 1036.
Helmke, J.P., Bauch, H.A., Röhl, U., Kandiano, E.S., 2008. Uniform climate development between the subtropical and subpolar northeast Atlantic across marine isotope stage 11. Clim. Past 4, 181–190.
Hemleben, C., Spindler, M., Anderson, O.R., 1989. Modern Planktonic Foraminifera. Springer, New York, pp. 1–363.
Hilgen, F.J., 1991. Astronomical calibration of Gauss to Matuyama sapropels in the Mediterranean and implication for the Geomagnetic Polarity Time Scale. Earth Planet. Sci. Lett. 104, 226–244.
Hilgen, F.J., Lourens, L.J., Berger, A., Loutre, M.F., 1993. Evaluation of the astronomically calibrated time scale for the late Pliocene and earliest Pleistocene. Paleoceanography 8, 549–565.
Hodell, D.A., Charles, C.D., Ninneman, U.S., 2000. Comparison of interglacial stages in the South Atlantic sector of the southern ocean for the past 450 ka: implications for marine isotope stage (MIS) 11. Glob. Planet. Chang. 24 (1), 7–26.
Hurrell, J.W., Hoerling, M.P., Phillips, A.S., Xu, T., 2004. Twentieth century North Atlantic climate change. Part I: assessing determinism. Clim. Dyn. 23, 371–389.
Imbrie, J., Imbrie, J.Z., 1980. Modeling the climatic response to orbital variations. Science 207, 943–953.
Incarbona, A., Di Stefano, E., Sprovieri, R., Bonomo, S., Censi, P., Dinarès-Turell, J., Spoto, S., 2008. Variability in the vertical structure of the water column and paleoproductivity reconstruction in the central-western Mediterranean during the Late Pleistocene. Mar. Micropaleontol. 69 (1), 26–41.
Insinga, D.D., Tamburrino, S., Lirer, F., Vezzoli, L., Barra, M., De Lange, G.J., Tiepolo, M., Vallefuoco, M., Mazzola, S., Sprovieri, M., 2014. Tephrochronology of the astronomically-tuned KC01B deep-sea core, Ionian Sea: insights into the explosive activity of the Central Mediterranean area during the last 200 ka. Quat. Sci. Rev. 85, 63–84.
Itambi, A.C., von Dobeneck, T., Mulitza, S., Bickert, T., Heslop, D., 2009. Millennial-scale northwest African droughts related to Heinrich events and Dansgaard–Oeschger cycles: evidence in marine sediments from offshore Senegal. Paleoceanography 24. http://dx.doi.org/10.1029/2007PA001570.
Jansen, J.H.F., Kuijpers, A., Troelstra, S.R., 1986. A Mid-Brunhes climatic event: Long term changes in global atmospheric and ocean circulation. Science 232, 619–622.
Johannessen, T., Jansen, E., Flatøy, A., Ravelo, A.C., 1994. The relationship between surface water masses, oceanographic fronts and paleoclimatic proxies in surface sediments of the Greenland, Iceland, Norwegian seas. In: Zahn, R., et al. (Eds.), Carbon Cycling in the Glacial Ocean: Constraints on the Ocean's Role in Global Change, NATO ASI Ser. I 117. Springer, Berlin, pp. 61–86.
Jouzel, J., Masson-Delmotte, V., Cattani, O., Dreyfus, G., Falourd, S., Hoffmann, G., Minster, B., Nouet, J., Barnola, J.M., Chappellaz, J., Fischer, H., Gallet, J.C., Johnsen, S., Leuenberger, M., Loulergue, L., Luethi, D., Oerter, H., Parrenin, F., Raisbeck, G., Raynaud, D., Schilt, A., Schwander, J., Selmo, E., Souchez, R., Spahni, R., Stauffer, B., Steffensen, J.P., Stenni, B., Stocker, T.F., Tison, J.L., Werner, M., Wolff, E.W., 2007.

Orbital and millennial Antarctic climate variability over the past 800,000 years. Science 317, 793–796.
Jullien, E., Grousset, F., Malaizé, B., Duprat, J., Sanchez-Goni, M.F., Eynaud, F., Charlier, K., Schneider, R., Bory, A., Bout, V., Flores, J.A., 2007. Low-latitude "dusty events" vs. high-latitude "icy Heinrich events". Quat. Res. 68 (3), 379–386.
Kallel, N., Paterne, M., Duplessy, J.C., Vergnaud-Grazzini, C., Pujol, C., Labeyrie, L., Arnold, M., Fontugne, M., Pierre, C., 1997. Enhanced rainfall in the Mediterranean region during the last sapropel event. Oceanol. Acta 20, 697–712.
Kandiano, E.S., Bauch, H.A., 2007. Phase relationship and surface water mass change in the NorthEast Atlantic duringMarine Isotope stage 11 (MIS11). Quat. Res. 68, 445–455.
Kandiano, E.S., Bauch, H.a., Fahl, K., Helmke, J.P., Röhl, U., Pérez-Folgado, M., Cacho, I., 2012. The meridional temperature gradient in the eastern North Atlantic during MIS11 and its link to the ocean–atmosphere system. Palaeogeogr. Palaeoclimatol. Palaeoecol. 333–334, 24–39.
Kawahata, H., 2005. Stable isotopic composition of two morphotypes of *Globigerinoides ruber* (white) in the subtropical gyre in the north Pacific. Paleontological Res. 9 (1), 27–35.
Klein, P., Coste, P., 1984. Effects of wind stress variability on nutrient transport into the mixed layer. Deep-Sea Res. 31, 21–37.
Konijnendijk, T.Y.M., Ziegler, M., Lourens, L.J., 2014. Chronological constraints on Pleistocene sapropel depositions from high-resolution geochemical records of ODP Sites 967 and 968. Newsl. Stratigr. 47 (3), 263–282.
Koutsodendris, A., Pross, J., Zahn, R., 2014. Exceptional Agulhas leakage prolonged interglacial warmth during MIS 11c in Europe. Paleoceanography 29, 1062–1071.
Krom, M.D., Kress, N., Brenner, S., Gordon, L.I., 1991. Phosphorus limitation of primary production in the eastern Mediterranean Sea. Limnol. Oceanogr. 36, 424–432.
Krom, M.D., Brenner, N.K., Neori, A., Gordon, L.I., 1992. Nutrient dynamics and new production in a warmcore eddy from the Eastern Mediterranean Sea. Deep-Sea Res. 39, 467–480.
Krom, M.D., Thingstad, T.F., Brenner, S., Carbo, P., Drakopoulos, P., Fileman, T.W., Flaten, G.A.F., Groom, S., Herut, B., Kitidis, V., Kress, N., Law, C.S., Liddicoat, M.I., Mantoura, R.F.C., Pasternak, A., Pitta, P., Polychronaki, T., Psarra, S., Rassoulzadegan, F., Skjoldal, E.F., Spyres, G., Tanaka, T., Tselepides, A., Wassmann, P., Wexels Riser, C., Woodward, E.M.S., Zodiatis, G., Zohary, T., 2005. Summary and overview of the CYCLOPS P addition Lagrangian experiment in the Eastern Mediterranean. Deep-Sea Res. II 52, 3090–3108.
Krom, M.D., Emeis, K.C., Van Cappellen, P., 2010. Why is the Eastern Mediterranean phosphorus limited? Prog. Oceanogr. 85, 236–244.
Kucera, M., 2007. Planktonic foraminifera as tracers of past oceanic environments. In: Hillaire-Marcel, C., de Vernal, A. (Eds.), Developments in Marine Geology, Volume 1, Proxies in late CenozoicPaleoceanography. Elsevier, pp. 213–262 (ISBN 13: 9780444527554).
Kuroyanagi, A., Kawahata, H., 2004. Vertical distribution of living planktonic foraminifera in the seas around Japan. Mar. Micropaleontol. 53, 173–196.
Kuroyanagi, A., Tsuchiya, M., Kawahata, H., Kitazato, H., 2008. The occurrence of two genotypes of the planktonic foraminifer *Globigerinoides ruber* (white) and paleoenvironmental implications. Mar. Micropaleontol. 68, 236–243.
Langereis, C.G., Dekkers, M.J., De Lange, G.J., Paterne, M., Van Santvoort, P.J.M., 1997. Magnetostratigraphy and astronomical calibration of the last 1.1 Myr from an eastern Mediterranean piston core and dating of short events in the Brunhes. Geophys. J. Int. 129, 75–94.
Laskar, J., Robutel, P., Joutel, F., Gastineau, M., Correia, A.C.M., Levrard, B., 2004. A Long-term Numerical Solution for the Insolation Quantities of the Earth: Astronomy and Astrophysics 428, 261–285.
Lin, H.L., Hsieh, H.Y., 2007. Seasonal variations of modern planktonic foraminifera in the South China Sea. Deep-Sea Res. II Top. Stud. Oceanogr. 54, 1634–1644.
Lin, H.L., Wang, W.C., Hung, G.W., 2004. Seasonal variation of planktonic foraminiferal isotopic composition from sediment traps in the South China Sea. Mar. Micropaleontol. 53 (3-4), 447–460.
Lionello, P., Malanotte-Rizzoli, P., Boscolo, R., Alpert, P., Artale, V., Li, L., Luterbacher, J., May, W., Trigo, R., Tsimplis, M., Ulbrich, U., Xoplaki, E., 2006. The Mediterranean climate: an overview of the main characteristics and issues. In: Lionello, P., Malanotte-Rizzoli, P., Boscolo, R. (Eds.), Mediterranean Climate Variability. Elsevier, Amsterdam, The Netherlands, pp. 1–26.
Lirer, F., Sprovieri, M., Ferraro, L., Vallefuoco, M., Capotondi, L., Cascella, A., Petrosino, P., Insinga, D., Pelosi, N., Tamburrino, S., Lubritto, C., 2013. Integrated stratigraphy for the Late Quaternary in the eastern Tyrrhenian Sea. Quat. Int. 292, 71–85.
Lirer, F., Sprovieri, M., Vallefuoco, M., Ferraro, L., Pelosi, N., Giordano, L., Capotondi, L., 2014. Planktonic foraminifera as bio-indicators for monitoring the climatic changes occurred during the last 2000 years in the SE Tyrrhenian Sea. Integrative Zool. J. 9, 542–554 (Lisiecki, L.E., Raymo, M.E., 2005. A Pliocene–Pliestocene stack of 57 globally distributed benthic d18O records. Paleoceanography 20, PA1003. doi:10.1029/2004PA001071).
Lisiecki, L.E., Raymo, M.E., 2005. A Pliocene–Pliestocene stack of 57 globally distributed benthic d18O records. Paleoceanography 20, PA1003. http://dx.doi.org/10.1029/2004PA001071.
Loewemark, L., Hong, W.L., Yui, T.F., Hung, G.W., 2005. A test of different factors influencing the isotopic signal of planktonic foraminifera in surface sediments from the northern South China Sea. Mar. Micropaleontol. 55 (1–2), 49–62.
Lourens, L.J., 2004. Revised tuning of Ocean Drilling Program Site 964 and KC01B (Mediterranean) and implications for the d18O, tephra, calcareous nannofossil, and geomagnetic reversal chronologies of the past 1.1 Myr. Paleoceanography 19 (PA3010).
Lourens, L.J., Hilgen, F.J., Zachariasse, W.J., van Hoof, A.A.M., Antonarakou, A., Vergnaud-Grazzini, C., 1996a. Evaluation of the plio-Pleistocene astronomical time scale. Paleoceanography 11, 391–413.
Lourens, L.J., Hilgen, F.J., Raffi, I., Vergnaud-Grazzini, C., 1996b. Early Pleistocene chronology of the Vrica section (Calabria, Italia). Paleoceanography 11, 797–812.
Loutre, M.F., 2003. Clues from MIS11 to predict the future climate—a modelling point of view. Earth Planet. Sci. Lett. 212, 213–224.
Luterbacher, J., Xoplaki, E., 2005. 500-year winter temperature and precipitation variability over the Mediterranean area and its connection to the large-scale atmospheric circulation. In: Bolle, H.-J. (Ed.), Mediterranean Climate. Variability and Trends. Springer Verlag, Berlin, New York, pp. 133–153.
Maiorano, P., Tarantino, F., Marino, M., De Lange, G.J., 2013. Paleoenvironmental conditions at Core KC01B (Ionian Sea) through MIS13–9: evidence from calcareous nannofossil assemblages. Quat. Int. 288, 97–111.
Malanotte-Rizzoli, P., Bergamasco, A., 1991. The wind and thermally driven circulation of the eastern Mediterranean Sea. Part II: The baroclinic case. Dyn. Atmos. Oceans 15, 355–419. http://dx.doi.org/10.1016/0377-0265(91)90026-C.
Malanotte-Rizzoli, P., Artale, V., Borzelli-Eusebi, G.L., Brenner, S., Crise, A., Gacic, M., Kress, N., Marullo, S., Ribera d'Alcalà, M., Sofianos, S., Tanhua, T., Theocharis, A., Alvarez, M., Ashkenazy, Y., Bergamasco, A., Cardin, V., Carniel, S., Civitarese, G., D'Ortenzio, F., Font, J., Garcia-Ladona, E., Garcia-Lafuente, J.M., Gogou, A., Gregoire, M., Hainbucher, D., Kontoyannis, H., Kovacevic, V., Kraskapoulou, E., Kroskos, G., Incarbona, A., Mazzocchi, M.G., Orlic, M., Ozsoy, E., Pascual, A., Poulain, P.M., Roether, W., Rubino, A., Schroeder, K., Siokou-Frangou, J., Souvermezoglou, E., Sprovieri, M., Tintoré, J., Triantafyllou, G., 2014. Physical forcing and physical/biochemical variability of the Mediterranean Sea: a review of unresolved issues and directions for future research. Ocean Sci. 10, 281–322.
Manca, B., Burca, M., Giorgetti, A., Coatanoan, C., Garcia, M.J., Iona, A., 2004. Physical and biochemical averaged vertical profiles in the Mediterranean regions: an important tool to trace the climatology of water masses and to validate incoming data from operational oceanography. J. Mar. Syst. 48, 83–116.
Marino, M., Maiorano, P., Tarantino, F., Voelker, A., Capotondi, L., Girone, A., Lirer, F., Flores, J.-A., Naafs, B.D.A., 2014. Coccolithophores as proxy of seawater changes at orbital-to-millennial scale during middle Pleistocene Marine Isotope Stages 14–9 in North Atlantic core MD01–2446. Paleoceanography 29 (6), 518–532.
Marino, G., Rohling, E.J., Rodrìguez-Sanz, L., Grant, K.M., Heslop, D., Roberts, A.P., Stanford, J.D., Yu, J., 2015. Bipolar seesaw control on last interglacial sea level. Nature 522, 197.
Martrat, B., Grimalt, J.O., Lopez-Martinez, C., Cacho, I., Sierro, F.J., Flores, J.A., Zahn, R., Canals, M., Curtis, J.H., Hodell, D.A., 2004. Abrupt temperature changes in the western Mediterranean over the past 250,000 years. Science 306, 1762–1765.
Masson-Delmotte, V., Kageyama, M., Braconnot, P., Charbit, S., Krinner, G., Ritz, C., Guilyardi, E., Jouzel, J., Abe-Ouchi, A., Crucifix, M., Gladstone, R.M., Hewitt, C.D., Kitoh, A., LeGrande, A.N., Marti, O., Merkel, U., Motoi, T., Ohgaito, R., Otto-Bliesner, B., Peltier, W.R., Ross, I., Valdes, P.J., Vettoretti, G., Weber, S.L., Wolk, F., Yu, Y., 2006. Past and future polar amplification of climate change: climate model intercomparisons and ice-core constraints. Clim. Dyn. 26, 513–529.
McManus, J.F., Oppo, D.W., Cullen, J.L., 1999. A 0.5 million year record of millennial-scale climate variability in the North Atlantic. Science 283, 971–974.
Milker, Y., Rachmayani, R., Weinkauf, M.F.G., Prange, M., Raitzsch, M., Schulz, M., Kucera, M., 2013. Global and regional sea surface temperature trends during Marine Isotope Stage 11. Clim. Past 9, 2231–2252.
Moreno, A., Cacho, I., Canals, M., Prins, M.A., Sánchez-Goñi, M.F., Grimalt, J.O., Weltje, G.J., 2002. Saharan dust transport and high latitude glacial climatic variability: the Alboran Sea record. Quat. Res. 58, 318–328.
Myers, P.G., Haines, K., Rohling, E.J., 1998. Modelling the paleo-circulation of the Mediterranean: the last glacial maximum and the Holocene with emphasis on the formation of sapropel S1. Paleoceanography 13, 586–606.
Napolitano, E., Oguz, T., Malanotte-Rizzoli, P., Yilmaz, A., Sansone, E., 2000. Simulations of biological production in the Rhodes and Ionian basins of the eastern Mediterranean. J. Mar. Syst. 24, 277–298.
Negri, A., Capotondi, L., Keller, J., 1999. Calcareous nannofossils, planktonic foraminifera and oxygen isotopes in the late Quaternary sapropels of the Ionian Sea. Mar. Geol. 157, 89–103.
Numberger, L., Hemleben, C., Hoffmann, R., Mackensen, A., Schulz, H., Wunderlich, J.-M., Kucera, M., 2009. Habitats, abundance patterns and isotopic signals of morphotypes of the planktonic foraminifer *Globigerinoides ruber* (d'Orbigny) in the eastern Mediterranean Sea since the Marine Isotopic Stage 12. Mar. Micropaleontol. 73 (1-2), 90–104.
Olausson, E., 1991. A post-Cromerian rise in sea level. In: Weller, G., Wilson, C.L., Severin, B.A.B. (Eds.), International Conference on the Role of Polar Regions in Global Change: Proceedings of a Conference Held Jun 11–15, 1990 at the University of Alaska Fairbanks vol. II. Geophysical Inst. Univ. of Alaska Fairbanks, pp. 496–498.
Oppo, D.W., McManus, J.F., Cullen, J.L., 1998. Abrupt climate events 500 000 to 340 000 years ago: evidence from subpolar North Atlantic sediments. Science 279, 1335–1338.
Perez-Folgado, M., Sierro, F.J., Flores, J.A., Cacho, I., Grimalt, J.O., Zahn, R., Shackleton, N.J., 2003. Western Mediterranean planktonic foraminifera events and millennial climatic variability during the last 70kyr. Mar. Micropaleontol. 48, 49–70.
Petit, J.R., Jouzel, J., Raynaud, D., Barkov, N.I., Barnola, J.M., Basile, I., Bender, M., Chappellaz, J., Davis, J., Delaygue, G., Delmotte, M., Kotlyakov, V.M., Legrand, M., Lipenkov, V., Lorius, C., Pépin, L., Ritz, C., Saltzman, E., Stievenard, M., 1999. Climate and atmospheric history of the past 420,000 years from the Vostok Ice Core, Antarctica. Nature 399, 429–436.
Pierre, C., Belanger, P., Saliège, J.F., Urrutiaguer, M.J., Murat, A., 1999. Paleoceanography of the western Mediterranean during the Pleistocene: oxygen and carbon isotope records at Site 975. Proc. Ocean Drill. Program Sci. Results 161, 481–488.
Pinardi, N., Masetti, E., 2000. Variability of the large-scale general circulation of the Mediterranean Sea from observations and modelling: a review. Palaeogeogr. Palaeoclimatol. Palaeoecol. 158, 153–173.
Piva, A., Asioli, A., Trincardi, F., Schneider, R.R., Vigliotti, L., 2008. Late-Holocene climate variability in the Adriatic Sea (Central Mediterranean). The Holocene 18 (1), 153–167.
Pujol, C., Vergnaud-Grazzini, C., 1989. Palaeoceanography of the last deglaciation in the Alboran Sea (western Mediterra- nean): stable isotopes and planktonic foraminiferal records. Mar. Micropaleontol. 15, 153–179.

Pujol, C., Vergnaud-Grazzini, C., 1995. Distribution patterns of live planktonic foraminuifers as related to regional hydrography and productive system of the Mediterranean Sea. Mar. Micropaleontol. 25, 187–217.
Reynolds, l.A., Thunell, R.C., 1986. Seasonal production and morphologic variation of *Neogloboquadrina pachyderma* (Ehrenberg) in the northeast Pacific. Micropaleontology 32, 1–18.
Roberts, A.P., Rohling, E.J., Grant, K.M., Larrasoaña, J.C., Liu, Q., 2011. Atmospheric dust variability from Arabia and China over the last 500,000 years. Quat. Sci. Rev. 30, 3537–3541.
Robinson, A.R., Golnaraghi, M., Leslie, W.G., Artegiani, A., Hecht, A., Lazzoni, E., Michelato, A., Sansone, E.A., Theocharis, A., Unluata, U., 1991. Structure and variability of the Eastern Mediterranean general circulation. Dyn. Atmos. Oceans 15, 215–240.
Rodrigues, T., Voelker, A.H.L., Grimalt, J.O., Abrantes, F., Naughton, F., 2011. Iberian Margin sea surface temperature during MIS15 to 9 (580–300 ka): glacial suborbital variability versus interglacial stability. Paleoceanography 26. http://dx.doi.org/10.1029/2010PA001927 (PA1204).
Roether, W.H., Manca, B.B., Klein, B., Bregant, D., Georgopoulos, D., Beitzel, V., Kovacevic, V., Luchetta, A., 1996. Recent changes in eastern Mediterranean deep waters. Science 271, 333–335.
Rogerson, M., Cacho, I., Jimenez-Espejo, F., Reguera, M.I., Sierro, F.J., Martinez-Ruiz, F., Frigola, J., Canals, M., 2008. A dynamic explanation for the origin of the western Mediterranean organic-rich layers. Geochem. Geophys. Geosyst. 9. http://dx.doi.org/10.1029/2007GC001936 (Q07U01).
Rohling, E.J., 1991. A simple two-layered model for shoaling of the eastern Mediterranean pycnocline due to glacio-eustatic sea level lowering. Paleoceanography 6, 537–541.
Rohling, E.J., 1994. Review and new aspects concerning the formation of eastern Mediterranean sapropels. Mar. Geol. 122, 1–28.
Rohling, E.J., De Rijk, S., 1999. The Holocene Climate Optimum and Last Glacial Maximum in the Mediterranean: the marine oxygen isotope record. Mar. Geol. 153, 57–75.
Rohling, E.J., Gieskes, W.W.C., 1989. Late Quaternary changes in Mediterranean intermediate water density and formation rate. Paleoceanography 4, 531–545.
Rohling, E.J., Jorissen, F.J., Vergnaud-Grazzini, C., Zachariasse, W.J., 1993. Northern Levantine and Adriatic Quaternary planktic foraminifera; reconstruction of paleoenvironmental gradients. Mar. Micropaleontol. 21, 191–218.
Rohling, E.J., Fenton, M., Jorissen, F.J., Bertrandt, P., Gans- sen, G., Caulet, J.P., 1998. Magnitudes of sea-level low- stands of the past 500,000 years. Nature 394, 162–164.
Rohling, E.J., Grant, K., Bolshaw, M., Roberts, A.P., Siddall, M., Hemleben, Ch., Kucera, M., 2009. Antarctic temperature and global sea level closely coupled over the past five glacial cycles. Nat. Geosci. 2, 500–504.
Rohling, E.J., Foster, G.L., Grant, K.M., Marino, G., Roberts, A.P., Tamisiea, M.E., Williams, F., 2014. Sea-level and deep-sea-temperature variability over the past 5.3 million years. Nature 508, 477–482.
Rohling, E.J., Marino, G., Grant, K.M., 2015. Mediterranean climate and oceanography, and the periodic development of anoxic events (sapropels). Earth Sci. Rev. 143, 62–97.
Rossignol-Strick, M., 1983. African monsoons, an immediate climate response to orbital insolation. Nature 30, 446–449.
Rossignol-Strick, M., Paterne, M., 1999. A synthetic pollen record of the eastern Mediterranean sapropels of the last 1 Ma: implications for the time-scale and formation of sapropels. Mar. Geol. 153, 221–237.
Rossignol-Strick, M., Paterne, M., Bassinot, F., Emeis, K.-C., DeLange, G.J., 1998. An unusual mid-Pleistocene monsoon period over Africa and Asia. Nature 392, 269–272.
Sanvoisin, R., D'Onofrio, S., Lucchi, R., Violanti, D., Castradori, D., 1993. 1 Ma Paleoclimatic Record from the Eastern Mediterranean Marflux Project: The First Results of Micropaleontological and Sedimentological Investigation of a Long Piston Core from the Calabrian Ridge. Il Quaternario. 6 pp. 169–188.
Sarmiento, J., Herbert, T., Toggweiler, J.R., 1988. Mediterranean nutrient balance and episodes of anoxia. Glob. Biogeochem. Cycles 2, 427–444.
Schiebel, R., Waniek, J.J., Matthias, B., Hemleben, C., 2001. Planktic foraminiferal production stimulated by chlorophyll redistribution and entrainment of nutrients. Deep Sea Research Part I. Oceanogr. Res. Pap. 48 (3), 721–740.
Schneider, T., Bischoff, T., Haug, G.H., 2014. Migrations and dynamics of the intertropical convergence zone. Nature 513, 45–53.
Seguenza, G., 1880. Le formazioni terziarie nella provincia di Reggio (Calabria): Rendiconti Accademia dei Lincei. Cl. Sci. Fis. Mat. Nat., Mem. 6 (3), 3–446 (tav. 1–17).
Shackleton, N.J., 1987. Oxygen isotopes, ice volume and sea level. Quat. Sci. Rev. 6, 183–190.
Siani, G., Paterne, M., Colin, C., 2010. Late Glacial to Holocene planktonic foraminifera bioevents and climatic record in the South Adriatic Sea. J. Quat. Sci. 25, 808–821.
Siegenthaler, U., Stocker, T.F., Monnin, E., Luethi, D., Schwander, J., Stauffer, B., Raynaud, D., et al., 2005. Stable carbon cycle–climate relationship during the late Pleistocene. Science 310, 1313–1317.
Sierro, F.J., Flores, J.A., Frances, G., Vazquez, A., Utrilla, R., Zamarreno, I., Erlenkeuser, H., Barcena, M.A., 2003. Orbitally-controlled oscillations in planktic communities and cyclic changes in western Mediterranean hydrography during the Messinian. Palaeogeogr. Palaeoclimatol. Palaeoecol. 190, 289–316.
Sierro, F.J., Hodell, D.A., Curtis, J.H., Flores, J.A., Reguera, I., Colmenero-Hidalgo, E., Bárcena, M.A., Grimalt, J.O., Cacho, I., Frigola, J., Canals, M., 2005. Impact of iceberg melting on Mediterranean thermohaline circulation during Heinrich events. Paleoceanography 20, PA2019. http://dx.doi.org/10.1029/2004PA001051.
Sprovieri, R., Di Stefano, E., Incarbona, A., Gargano, M.E., 2003. A high- resolution record of the last deglaciation in the Sicily Channel based on foraminifera and calcareous nannofossil quantitative distri-bution. Palaeogeogr. Palaeoclimatol. Palaeoecol. 202, 119–142.
Sprovieri, M., Di Stefano, E., Incarbona, A., Salvagio Manta, D., Pelosi, N., Ribera d'Alcalà, M., Sprovieri, R., 2012. Centennial to millennial scale climate oscillations in the Central Eastern Mediterranean Sea between 20,000 and 70,000 years ago: evidence from a high-resolution geochemical and micropaleontological record. Quat. Sci. Rev. 46, 126–135.
Stefanelli, S., Capotondi, L., Ciaranfi, N., 2005. Foraminiferal record and environmental changes during the deposition of the early–middle Pleistocene sapropels in southern Italy. Palaeogeogr. Palaeoclimatol. Palaeoecol. 216, 27–52.
Stein, R., Hefter, J., Grützner, J., Voelker, A., Naafs, B.D.A., 2009. Variability of surface water characteristics and Heinrich-like events in the Pleistocene midlatitude North Atlantic Ocean: biomarker and XRD records from IODP Site U1313 (MIS16-9). Paleoceanography 24. http://dx.doi.org/10.1029/2008PA001639.
Thirumalai, K., Richey, J.N., Quinn, T.M., Poore, R.Z., 2014. *Globigerinoides ruber* morphotypes in the Gulf of Mexico: a test of null hypothesis. Sci. Rep. 4, 6018.
Thunell, R.C., 1978. Distribution of recent planktonic foraminifera in surface sediments of the Mediterranean Sea. Mar. Micropaleontol. 3, 147–173.
Thunell, R.C., Poli, M.-S., Rio, D., 2002. Changes in deep and intermediate water properties in the western North Atlantic during marine isotope stages 11–12: evidence from ODP Leg 172. Mar. Geol. 189, 63–77.
Triantaphyllou, M.V., Ziveri, P., Gogou, A., Marino, G., Lykousis, V., Bouloubassi, I., Emeis, K.C., Kouli, K., Dimizia, M., Rosell-Mele, A., Papanikolaou, M., Katsouras, G., Nunez, N., 2009. Late GlacialeHolocene climate variability at the south-eastern margin of the Aegean Sea. Mar. Geol. 266, 182–197.
Trigo, R.M., Pozo-Vazquez, D., Osborn, T.J., Castro-Dıez, Y., Gamiz-Fortis, S., Esteban-Parra, M.J., 2004. North Atlantic oscillation influence on precipitation, river flow and water resources in the Iberian Peninsula. Int. J. Climatol. 24, 925–944.
Tzedakis, P.C., 2010. The MIS 11—MIS 1 analogy, southern European vegetation, atmospheric methane and the early anthropogenic hypothesis. Clim. Past 6, 131–144.
Tzedakis, P.C., Channell, J.E.T., Hodell, D.A., Kleiven, H.F., Skinner, L.C., 2012. Determining the natural length of the current interglacial. Nat. Geosci. 5, 138–141.
van Santvoort, P.J.M., De Lange, G.J., Langereis, C.G., Dekkers, M.J., 1997. Geochemical and paleomagnetic evidence for the occurrence of "missing" sapropels in eastern Mediterranean sediments. Paleoceanography 12 (6), 773–786.
Voelker, A.H.L., Rodrigues, T., Hefter, J., Billups, K., Oppo, D., McManus, J., Stein, R., Grimalt, J.O., 2010. Variations in mid-latitude North Atlantic surface water properties during the mid-Brunhes (MIS9–14) and their implications for the thermohaline circulation. Clim. Past 6, 531–552.
Wang, L.J., 2000. Isotopic signals in two morphotypes of *Globigerinoides ruber* (white) from the South China Sea: implications for monsoon climate change during the last glacial cycle. Palaeogeogr. Palaeoclimatol. Palaeoecol. 161 (3–4), 381–394.
Wang, Y.J., Cheng, H., Edwards, R.L., An, Z.S., Wu, J.Y., Shen, C.C., Dorale, J.A., 2001. A high-resolution absolute-dated late Pleistocene monsoon record from Hulu Cave, China. Science 294, 2236–2239.
Ziveri, P., Rutten, A., de Lange, G.J., Thomson, J., Corselli, C., 2000. Present-day coccolith fluxes recorded in central Eastern Mediterranean sediment traps and surface sediments. Palaeogeogr. Palaeoclimatol. Palaeoecol. 158, 175–195.